Decarbonization of gas transmission pipelines via hydrogen blending: A Techno-Environmental case study approach

Pronob Das, Md. Shahriar Mohtasim, Andrew Rowe, & Peter Wild

2025

Original citation:
Das, P., Mohtasim, Md. S., Rowe, A., & Wild, P. (2026). Decarbonization of gas transmission pipelines via hydrogen blending: A Techno-Environmental case study approach. *Energy Conversion and Management*, *351*, Article 121010.
https://doi.org/10.1016/j.enconman.2025.121010

Energy Conversion and Management 351 (2026) 121010

Contents lists available at ScienceDirect

Energy Conversion and Management

journal homepage: www.elsevier.com/locate/enconman

Decarbonization of gas transmission pipelines via hydrogen blending: A Techno-Environmental case study approach

Pronob Das [a,b,*], Md. Shahriar Mohtasim [b], Andrew Rowe [a], Peter Wild [a]

[a] Institute for Integrated Energy Systems (IESVic), University of Victoria, PO Box 1700 STN CSC, Victoria, BC V8W 2T2, Canada
[b] Department of Mechanical Engineering, Rajshahi University of Engineering & Technology, Rajshahi 6204, Bangladesh

ARTICLE INFO

Keywords:
Natural gas pipeline
Hydrogen blending
Decarbonization
Compressor electrification
Energy return on investment

ABSTRACT

This study presents a novel and validated optimization framework to evaluate the performance and techno-environmental and economic impacts of hydrogen blending in steady-state natural gas transmission pipelines. The model investigates hydrogen injection (0 %, 10 %, 20 % and 100 %) and its influence on key parameters, including flow behavior, compressor fuel consumption, pressure limits, emissions, and energy return on investment (EROI). Using a genetic algorithm (GA) implemented in MATLAB, the framework is applied to both generalized cases and a real commercial system, the Coastal GasLink pipeline in Canada. Hydrogen addition significantly alters system behavior, increasing maximum operating pressure from 6.9 to 8.2 MPa and raising compressor fuel use from 2.98 % (100 % NG) to 21.4 % (100 % H_2) over an 800 km pipeline. Validation against multiple benchmark studies shows < 1.5 % deviation, confirming model reliability. The study introduces a cost and emission trade-off analysis using a marginal abatement cost curve to assess compressor station electrification strategies. Full electrification reduces emissions by 1.51 $MtCO_2$/year but increases operating costs. However, under Canadian incentive structures, the cost of abatement decreases substantially, making large-scale emission reduction economically viable. The analysis also highlights a sharp decline in EROI from 33.56 (100 % NG) to 4.67 (100 % H_2), underscoring the need for efficiency-focused infrastructure design. A forward-looking hybrid energy system is proposed, integrating renewables, battery storage, and electrolyzers to enable on-site green hydrogen production and electrified compression. This framework supports infrastructure planning aligned with national decarbonization goals for 2030 and beyond.

1. Introduction

The escalating consequences of climate change demand urgent action to mitigate greenhouse gas (GHG) emissions, spurring a worldwide move towards cleaner energy systems [1]. Among various transition pathways, hydrogen (H_2) has emerged as a pivotal vector for decarbonization, owing to its high gravimetric energy density and potential for zero-carbon combustion [2]. However, the absence of widespread H_2-specific infrastructure remains a critical challenge for its integration into current energy systems. In this context, blending H_2 into existing natural gas (NG) transmission networks has been recognized as a promising near-term strategy to incrementally scale H_2 deployment while leveraging mature pipeline infrastructure [3].

NG continues to dominate global energy supply, accounting for nearly 23 % of primary energy consumption, and is projected to expand further in several regional markets by mid-century [1,4]. The world's extensive NG pipeline infrastructure, crucial for transporting over 90 % of supply, provides a ready-made logistical foundation. However, its traditional design is increasingly challenged due to the substantial energy required for compression and the emissions this generates [5,6]. Furthermore, the decarbonization of such networks calls for innovative operational strategies, including fuel consumption minimization and electrification of compressor stations [7].

The integration of H_2 into the NG system complicates pipeline management. Operational issues arise from modified flow patterns and alter physical properties such as viscosity, compressibility, and calorific value [8,9]. These changes fundamentally impact pressure drop, compressor power demand, and permissible operating pressures (MAOP), with consequences for both system functionality and cost-effectiveness. Modeling these hybrid H_2-NG systems requires an integrated understanding of gas dynamics, safety margins, and optimization techniques that accommodate nonlinearities and constraints inherent in large-scale energy infrastructure [10].

* Corresponding author at: Department of Mechanical Engineering, University of Victoria, Victoria, BC V8W 2T2, Canada.
E-mail address: pronobdasruet@gmail.com (P. Das).

https://doi.org/10.1016/j.enconman.2025.121010
Received 15 June 2025; Received in revised form 20 December 2025; Accepted 26 December 2025
Available online 29 December 2025

Nomenclature

A	Area, m^2
c	Sonic velocity, m/s
CH_4	Methane gas
CO_2	Carbon-di-oxide gas
C_p	Specific heat capacity at constant pressure, J/kmol.K
C_v	Specific heat capacity at constant volume, J/kg·K
D	Pipeline internal diameter, m
f	Darcy friction factor
f_E	Seam joint factor
f_F	Design factor
f_T	Temperature direction factor
g	Gravity acceleration, m/s^2
h	Compressor isentropic head, KJ/kg
H_2	Hydrogen gas
k	Isentropic exponent
L	Pipeline length, km
M	Molecular mass, g/mol
m	Mass flow rate, kg/s
m_d	Delivered mass flow rate, kg/s
m_f	Compressor fuel consumption rate, kg/s
n_c	Number of compressors
P	Compressor required power, kw
p	Average pressure, Pa
P_b	Base pressure, kPa
P_c	Pseudo critical pressure, Pa
p_d	Delivery pressure, Pa
P_r	Reduced pressure, Pa
p_s	Supply pressure, Pa
Q	Volumetric flow rate, m^3/s
R	Universal gas constant, 8314 J/kmol-K
t	Pipe wall thickness, m
T	Temperature, K
T_c	Pseudo critical temperature, K
T_r	Reduced temperature, K
V	Gas velocity, m/s
v_e	Erosional velocity, m/s
Z	Compressibility factor
η_d	Driver efficiency, %
η_i	Isentropic efficiency, %
η_m	Mechanical efficiency, %
ε	Material roughness, μm
ρ	Density, kg/m^3

Acronyms

ACO	Ant Colony Optimization
CFC	Compressor fuel consumption
CFR	Clean fuel regulations
EROI	Energy return on investment
EIR	Energy intensity ratio
GA	Genetic algorithm
GHG	Greenhouse gas
GRG	Generalized reduced gradient
HHV	Higher heating value, kJ/kg
LHV	Lower heating value, kJ/kg
MAC	Marginal abatement cost
MACC	Marginal abatement cost curve
MAOP	Maximum allowable operating pressure
MILP	Mixed-integer linear programming
NG	Natural gas
NPS	Nominal pipe size
P2H	Power-to-H_2
PSO	Particle swarm optimization
Re	Reynolds number
SMYS	Stipulated minimum yield strength

Recent advancements in optimization algorithms, including genetic algorithms (GA), ant colony optimization (ACO), and particle swarm optimization (PSO), have demonstrated considerable potential in enhancing pipeline efficiency and reducing compressor fuel consumption [3,11]. However, few studies have fully integrated H_2 blending dynamics with compressor station electrification, an increasingly viable decarbonization strategy as electricity grids become cleaner through renewable integration [12]. Electrifying compressors can drastically cut CO_2 emissions, especially in regions with low-carbon electricity generation, albeit at higher operational costs. It is imperative for developing system-level models that surpass theoretical estimations and offer dependable, validated tools for evaluating the operational feasibility and optimization of H_2-enriched NG pipelines. This becomes even more critical as countries like Canada, Germany, and Japan adopt H_2 roadmaps that heavily rely on repurposing existing NG infrastructure to reduce cost and deployment time.

Canada's national H_2 strategy, released in December 2020, positions H_2 as a critical component for achieving net-zero emissions by 2050, targeting H_2 to supply up to 30 % of the country's end-use energy by that date [13–15]. The strategy emphasizes leveraging Canada's clean electricity and natural resources to produce low-carbon H_2 (blue and green), aiming to create domestic and export markets while stimulating economic growth. Aligning with this federal vision, British Columbia's CleanBC plan sets ambitious provincial targets, including a 40 % reduction in greenhouse gas emissions below 2007 levels by 2030 and achieving net-zero emissions by 2050 [16]. CleanBC specifically identifies renewable gases, including H_2, as essential solutions for decarbonizing hard-to-abate sectors like industry, heavy-duty transport, and building heat, with an interim target of 15 % renewable gas content in the NG system by 2030 [16]. Together, these strategies create a synergistic framework, recognizing H_2's vital role in addressing emissions where direct electrification is challenging and driving clean technology investment across the country and within BC [17,18]. Table 1 provides a comprehensive literature review on H_2-blended NG pipeline optimization.

Fig. 1 shows a bibliometric mapping that summarizes current research trends in H_2-NG blending. The network discovers many major topic clusters by analyzing keyword co-occurrences in relevant literature. The center node, "H_2" connects to significant keywords such as NG, renewable energy, power-to-gas, and underground H_2 storage, emphasizing the multifaceted integration of H_2 into current energy systems. The blue cluster, which includes keywords like pipeline, dynamic simulation, transient flow, and genetic algorithm, focuses on modeling techniques and transient flow behavior in gas pipeline networks. In parallel, the purple cluster, with keywords like H_2-blended NG pipeline, compressor electrifications, numerical simulation, and mixing uniformity, points to the growing interest in CFD-based studies, safety considerations, and power consumption. The red and orange clusters collectively focus on decarbonization pathways, including green H_2, electrolyzers, and integrated energy systems, underscoring the shift toward clean H_2 integration in power and industrial sectors.

Another notable theme area is represented by the green cluster, which focuses on subsurface H_2 storage and includes phrases like depleted gas reservoir, diffusion, leakage, and reservoir simulation. This implies a growing interest in seasonal and large-scale H_2 storage solutions. Despite substantial technical study, the existence of optimization and simulation in the network suggests a relatively underrepresented but growing demand for performance-based validation models that take

Table 1
Comprehensive literature review on H_2-blended NG pipeline optimization.

Ref.	Focus Area	Methodology	Key Findings	Limitations
[10]	NG with H_2 blending (27.3 %)	Non-linear optimization	Each 1 % H_2 added to the NG network reduced cost by ~ 3.29 %, lowering total cost from M $24.78 to M $22.23 and emissions by 11.48 % (11.84 to 10.63 $ktCO_2$).	The study does not detail system-level constraints or integration with real-time operation scenarios.
[19]	NG with H_2 blending (max 9.85 %-mol)	Simulation (ACO)	Ant colony optimization found that up to 9.85 % H_2 can be blended while delivering 8420 MJ and keeping compressor fuel use at 1.01 kg/s, proving efficient, low-fuel H_2 injection is feasible.	The model considers static conditions and does not analyze dynamic operational uncertainties.
[8]	NG with H_2 blending (30 %)	Simulation	A 30 % H_2 blend cut emissions by 36.3 %, but increasing to 60 % reduced energy efficiency by 35 %, revealing a trade-off between emissions reduction and energy delivery.	The simulation did not analyze system reliability or material compatibility under higher H_2 blends.
[20]	NG with H_2 blending (30 %)	Simulation (ASPEN)	ASPEN simulation showed single-point H_2 injection reduced pressure drops, while multi-point injection increased them, highlighting the injection strategy's impact on system efficiency.	The study lacks insight into long-distance network effects and time-based load variations.
[21]	NG with H_2 blending (10 %)	Simulation (MILP)	Mixed-integer linear programming showed a 10 % H_2 blend raises pipeline costs, indicating economic sensitivity at low blend levels.	Emissions and energy efficiency impacts were not evaluated.
[22]	NG only	Simulation (MILP)	Simulation of a pure NG network using MILP showed a cost reduction of approximately 7.5 %, illustrating the effectiveness of optimization techniques for cost minimization in traditional NG systems.	The study does not consider future adaptation to H_2 or hybrid systems.
[23]	NG only	Simulation (MILP)	Optimized NG pipeline configuration reduced costs and improved efficiency, highlighting the economic benefit of linear optimization in gas transmission.	H_2 integration scenarios were not explored.
[1]	H_2 blending in NG pipelines, compressor electrification, fuel/emission optimization	GA-optimized isothermal gas flow modeling of an 800 km pipeline with multiple deliveries using MATLAB	H_2 blending (5 %–20 %) reduces CO_2 emissions by 2 %–6%, electrification of compressors reduces emissions from 430 to 32 $ktCO_2$/year but raises costs from M$15 to M $178/year.	Lack of economic and energy-based analysis, absence of validation.
[24]	Feasibility and risks of H_2 blending in existing NG networks	Hydraulic modeling and Real-Time Transient Modeling applied to transmission and distribution pipelines.	Simulated up to 100 % H_2 blends, identified safety risks (e.g., flammability, embrittlement), developed compatibility strategies for compressors, and showed GHG reduction potential even considering H_2 production.	The study did not conduct cost optimization and assumed simplified pipe materials and boundary conditions, excluding distribution lines from compression modeling.
[25]	Leak detection	Analytical modeling	Fast leak location via pressure wave dynamics.	Model validation with field data is lacking.
[26]	Material safety with H_2 blending	Literature review	Identified risks like embrittlement and fatigue.	No experimental validation.
[27]	CFD modeling of NG-H_2 blend	Transient and steady-state CFD	H_2 increases the pressure drop and compressor load.	Small-scale validation only.
[28]	Pipeline routing optimization	Multi-objective modeling	Balanced cost, safety, and environment in routing.	Ignores H_2-specific effects.
[29]	Renewable gas injection	Multi-period optimization	M$12 savings by optimal H_2 injection.	Based on static grid prices.
[30]	Energy metering integration	Optimization model	Real-time metering enhances decisions.	Limited to distribution networks.
[31]	HENG flow estimation	Graph-enhanced DeepONet AI	Achieves real-time flow prediction under dynamics.	Needs robust training datasets.
[32]	Pipeline conversion to 100 % H_2	Thermodynamic modeling	Significant redesign needed for full H_2.	No cost analysis included.

(continued on next page)

Table 1 (*continued*)

Ref.	Focus Area	Methodology	Key Findings	Limitations
[33]	Energy capacity of H_2 blends	Novel empirical equations	H_2 lowers energy transfer capacity.	Idealized network assumptions.
[34]	H_2 blending in residential grid	Simulation analysis	≤10 % H_2 viable in appliances with minor change.	Not generalized to industry.
[35]	Hydraulic and thermal effects	Simulation of flow + temp	H_2 affects pressure/heat transfer significantly.	Simplified pipe geometry.
[36]	H_2 in NG and smart grids	Review study	Shows synergy potential in future energy systems.	Blending limit data is still scarce.

into account both engineering restrictions and economic feasibility. In this context, the optimization and validation of an NG transmission pipeline with H_2 injection effect becomes a crucial area of research, as it bridges technical simulation with practical deployment. Accurate modeling and validation ensure system reliability, safety, and performance under varying H_2 blending ratios, which is key to enabling scalable H_2-NG integration in existing infrastructures.

The objective of this study is, therefore, to fill this urgent knowledge gap by developing a robust framework that enables the performance optimization and techno-economic evaluation of NG pipelines under H_2 injection scenarios, while also supporting decision-making for infrastructure retrofitting, emissions reduction, and grid decarbonization. Such a holistic and data-driven approach is essential for ensuring that H_2 blending can be implemented safely, efficiently, and in alignment with national and international H_2 energy strategies, making this study not only timely but fundamentally necessary within these scopes. The main contributions of the study are as follows,

- The study presents a first-of-its-kind optimization framework that integrates H_2 injection effects into steady-state NG transmission pipeline modeling of single delivery. Unlike prior studies focusing solely on NG or simplified H_2 blending, this model quantitatively evaluates hydrogen's impact on pressure, flow, fuel consumption, and MAOP over varying compositions (0 %, 10 %, 20 % and 100 % of H_2), which is highly relevant to the decarbonization goals.
- The study pioneers a cost-emission trade-off framework for compressor station electrification under different H_2 blending scenarios. Through Marginal Abatement Cost Curve (MACC) analysis, it quantifies economic and environmental outcomes of hybrid and full electrification, supporting Canada's 2030 climate goals. This is particularly novel and urgent in light of energy transition policies.
- Unlike most pipeline studies, this work incorporates EROI and energy intensity ratio analyses under different H_2 blending ratios. The declining EROI trend with higher H_2 content is quantified and contextualized, offering an energy intensity perspective that is rare in pipeline optimization literature.
- A major highlight is the application of the proposed model to a real commercial pipeline, Coastal GasLink (Canada). This empirical application connects theoretical optimization with practical constraints (diameter, MAOP, flow demand), offering policy-relevant insights that are often lacking in purely theoretical studies.

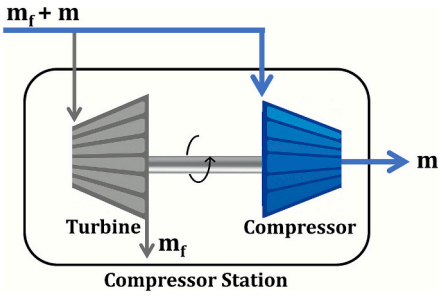

Fig. 2. A centrifugal compressor and turbine arrangement within a compressor station.

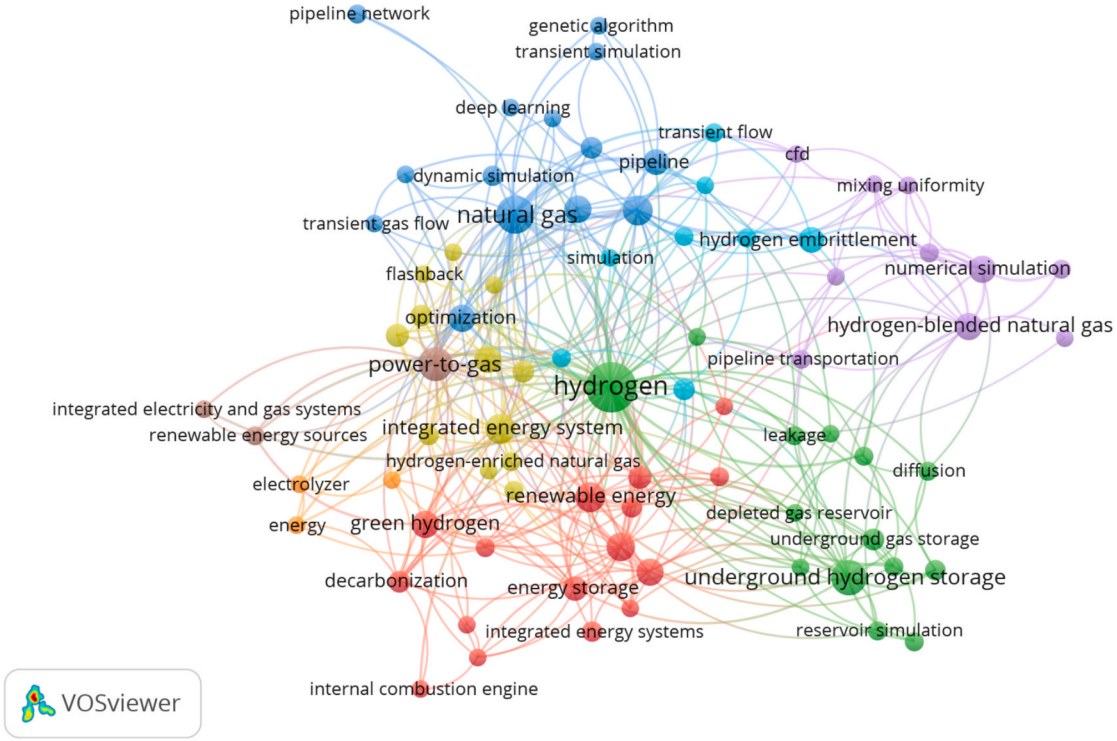

Fig. 1. A bibliometric map highlighting current research trends in H_2-NG blending.

- A future-oriented section introduces a modular hybrid system combining renewables, battery storage, and electrolyzers to enable on-site green H_2 production and injection, while simultaneously electrifying compressors. This dual-purpose energy system represents an innovative convergence of H_2 and renewable power integration.

2. Methodology

2.1. Mathematical modeling

The flow of NG through a pipeline is governed by fluid dynamics principles, incorporating the conservation of mass, momentum, and energy. The fundamental flow equation is derived from partial differential equations. This study considers a steady-state, isothermal flow, assuming no elevation changes in the pipeline. All the required equations for the NG pipeline optimization are stated in Table 2.

For hydrogen–natural gas blends, hydrogen is explicitly treated as an additional component in the gas mixture. For each hydrogen blending ratio, the mixture's pseudo-critical temperature and pressure are recalculated using mole-fraction-weighted mixing rules (Kay's rule), which account for the critical properties of both natural gas components and hydrogen. The resulting pseudo-reduced pressure and temperature are then used in the DPR correlation to evaluate the compressibility factor. Consequently, the compressibility factor varies with hydrogen blending ratio, pressure, and temperature.

2.2. Objective function

The choice of objective functions varies with the problem definition and may involve optimizing the network's design or enhancing the operational efficiency of the gas network. As shown in Table 1, the majority of researchers have focused on minimizing compressor fuel consumption as a key objective in the optimization process. This approach is directly linked to reducing emissions and overall energy consumption. In this study, the objective function, f, is formulated as follows, where n_c represents the number of compressor stations in the pipeline:

$$f = \min \sum_{1}^{n_c} m_f \tag{21}$$

The total fuel consumption across all compressor stations is determined by summing the fuel consumption of individual compressors.

2.3. Optimization process

Natural gas transmission systems are highly complex by nature. For practical modeling and optimization, these pipeline networks are usually represented in a simplified form consisting of three key elements: pipelines, compressor stations, and terminals. Because pipelines handle massive amounts of natural gas, even slight decreases in fuel use at compressor stations can lead to considerable resource savings. Thus, optimizing operating parameters to lower energy consumption is essential for achieving efficient and sustainable gas transmission. To tackle this issue, researchers have proposed a range of optimization approaches focused on reducing fuel consumption. Recent studies have explored methods such as GA, ACO, and Generalized Reduced Gradient (GRG) for different applications in NG network optimization [6]. Based on a comprehensive literature review, GA was chosen to optimize the present model due to its flexibility, robustness, and efficiency in handling complex, multi-dimensional, and constrained systems, as shown in Fig. 3 **(a).** GA has been widely recognized as an effective approach for optimizing NG pipeline operations, particularly in minimizing compressor fuel consumption. Prior studies have demonstrated its capability to enhance energy efficiency in gas compressor plants. Furthermore, several studies have explored the application of GA in optimizing gas network workflows [19].

Fig. 3 **(b)** illustrates the comprehensive GA algorithm. In this approach, a population size of 200 and a maximum of 500 iterations are utilized. A sufficiently large population size ensures diversity among candidate solutions, which reduces the risk of premature convergence and improves the algorithm's ability to explore the global search space. At the same time, limiting the iterations prevents excessive computational time while still allowing adequate refinement of solutions. The total number of fitness function evaluations, calculated as the product of population size and maximum iterations, increases the likelihood of approaching the global optimum in a highly nonlinear and multi-constraint pipeline optimization problem. Generally, a higher number of evaluations increases the likelihood of discovering superior solutions, whereas lower values may reduce this probability.

The selected crossover and mutation rates of 0.8 and 0.2, respectively, were chosen based on their demonstrated effectiveness compared to other parameter combinations. When the crossover probability is set to 0.8, meaning that 80 % of the offspring inherit characteristics from two parents. A high crossover rate accelerates convergence by recombining promising features of existing solutions, which is particularly beneficial for problems with complex interdependencies such as gas flow and compressor dynamics. The mutation probability was set to 0.2 to introduce controlled randomness into the population, preventing stagnation in local optima and maintaining diversity throughout the search. These values were chosen after preliminary sensitivity testing and are consistent with previous optimization studies on gas transmission systems [6,19], where similar parameter ranges demonstrated stable convergence and superior solution quality compared to other configurations. For a detailed explanation of the GA methodology, readers are referred to reference [1].

3. Gas pipeline network model

The general workflow of the study is illustrated in Fig. 4**.** It begins with oil and gas extraction from wells, followed by the separation of oil, gas, and water. The separated gas is sent to a processing facility, where non-hydrocarbon components are removed, and certain by-products are either vented, flared, or reinjected into the field. After processing, the natural gas is compressed at compressor stations to maintain efficient flow through the pipeline system. For this study, the inlet gas pressure from the processing plant to the first compressor is assumed to be 1.38 MPa (200 psi).

A simple 800 km gas transmission system is considered for this study, as shown in Fig. 5, which illustrates a simplified and idealized network developed for methodology demonstration. The system assumes uniform pipeline geometry, evenly spaced compressor stations, and simplified boundary conditions to enable transparent analysis of parameter interactions. This model is not intended to represent any specific real-world pipeline but serves as a baseline configuration for developing the proposed optimization approach. Eight compressor stations are considered along this pipeline, where all are single-stage compressors, except the first compressor. The distance between adjacent compressors is 100 km. There are eight pipeline arcs (G1-G8) in the transmission line with sixteen nodes. Initially, gas comes from the gas processing plant at 1.38 MPa to the first compressor. After that, the gas is compressed at the first compressor and goes forward to the other compressors towards the delivery node (node 16). The pipeline diameter is 0.9 m, and the operating pressure of the pipeline is maintained below the maximum allowable operating pressure (MAOP), which is calculated to be 8.6 MPa for a 0.9 m pipeline. Additionally, the delivery pressure at node 16 is assumed to be equal to or greater than 1.38 MPa.

The natural gas composition used in this study was adopted from recent data reported for the LNG Canada project in British Columbia. The natural gas composition (on a molar basis) consisted of 95.27 % methane (CH_4), 0.41 % ethane (C_2H_6), 0.094 % propane (C_3H_8), 0.014

Table 2
Commonly used equations to optimize the NG transmission pipeline with constraints.

Equation Name	Description	Equation	Parameters	Eqn. no.
Pipe flow equation	The steady-state pressure drop in a horizontal pipeline is determined by equation (1), which is derived under the assumptions of isothermal conditions and a constant compressibility factor between the inlet and outlet. This formulation is selected due to its rigorous treatment of compressible gas flow under steady-state conditions, ensuring precise quantification of frictional losses. Unlike simplified or empirically derived models such as the Darcy–Weisbach, Weymouth, or Panhandle equations, this approach provides enhanced accuracy by explicitly incorporating thermodynamic and fluid dynamic principles governing compressible flow [19].	$({P_2}^2 - {P_1}^2) - \frac{32m^2ZRT}{\pi^2D^4M}\log_{10}\left(\frac{P_2}{P_1}\right) + \frac{16f}{\pi^2D^5}\frac{ZRT}{M}m^2L = 0$	P_1 = Upstream pressure of the pipe (Pa) P_2 = Downstream pressure of the pipe (Pa) m = Mass flow rate in the pipeline (kg/s) R = Universal gas constant = $8.314\ \frac{J}{mol.K}$ T = Gas temperature (K) D = Inner Diameter of pipeline (m) M = Molecular mass of gas ($\frac{kg}{mol}$) L = Length of the pipe (m)	(1)
Friction factor	The friction factor can be determined using the Prandtl-von Kármán equation, which establishes a direct dependence on the relative roughness of the pipeline. This simplification is justified under fully developed turbulent flow conditions, a characteristic regime in gas transmission pipelines. While the Colebrook-White equation provides a more generalized approach by incorporating both Reynolds number and relative roughness, its implicit nature necessitates iterative numerical solutions. Consequently, the Prandtl-von Kármán formulation offers a computationally efficient alternative when flow conditions are sufficiently turbulent to justify neglecting Reynolds number effects [6,19].	$f = -2\log_{10}\left(\frac{\varepsilon}{3.71 \times D}\right)^{-2}$	ε = Pipeline material roughness (m)	(2)
Fuel consumption of compressor (kg/s)	Centrifugal compressors in pipeline systems are typically driven by electric motors, steam turbines, or internal combustion engines. In the case of turbine-driven compressors, a portion of the transported NG is utilized as fuel to power the compression process. These compressors employ an impeller mechanism to increase the gas pressure along the pipeline [6,19]. This study focuses on NG turbine-driven centrifugal compressors, fueled by product stream extraction, rather than electrically driven alternatives, as shown in Fig. 2. The power requirement for compression (P) is determined by accounting for mechanical efficiency (η_m), driver efficiency (η_d), and the lower heating value (LHV) of the fuel. These parameters collectively define the fuel consumption rate for each compressor, as expressed in equation (3).	$m_f = \frac{mh_i}{\eta_i\eta_m\eta_d LHV}$	h_i= Compressor isentropic head (kJ/kg) LHV = Lower heating value of gas (kJ/kg) η_i = Isentropic efficiency of the compressor η_m = Mechanical efficiency of the compressor η_d = Driver efficiency	(3)
Lower heating value (kJ/kg)	Compressor stations typically consume 3 %–5% of the transported NG as fuel. The compression process is characterized by three key efficiency parameters: The fuel consumption calculation incorporates the LHV, defined as the maximum energy released per unit mass during complete combustion. For accurate computation, the mass-specific LHV (LHV_i) of each gas component is evaluated at standard conditions (25 °C, 1 bar) and expressed in kJ/kg [19,37]. • Isentropic efficiency: 0.72 • Mechanical efficiency: 0.90 • Driver efficiency: 0.35	$\text{LHV} = \frac{\sum y_i M_i LHV_i}{\sum y_i M_i}$	y_i = Mole fraction of individual gases	(4)
Compressor isentropic head (kJ/kg)	Compressors increase the pressure of NG as it flows through the pipeline. The isentropic head, a key parameter in compression analysis, represents the theoretical work input required per unit mass to raise the gas pressure from suction conditions to discharge pressure under adiabatic (isentropic) conditions.	$h_i = \frac{ZRT}{M}\frac{k}{k-1}\left[\left(\frac{p_d}{p_s}\right)^{\frac{k-1}{k}} - 1\right]$	k = Isentropic exponent (~1.3) p_d = Delivery pressure from compressor (Pa) p_s= Supply pressure to compressor (Pa)	(5)
Compressor required power (kW) [38]	The power necessary to drive the compressor in kW is determined with this equation.	$\text{P} = \frac{mh_i}{\eta_i}$		(6)

(continued on next page)

Table 2 (*continued*)

Equation Name	Description	Equation	Parameters	Eqn. no.
Compressibility factor	To accurately model gas compression behavior, the ideal gas law is modified by introducing the compressibility factor (Z), which accounts for deviations from ideality. In this study, the Dranchuk-Purvis-Robinson (DPR) equation is employed to determine Z. The pseudo-critical properties of NG are derived from the critical properties of its individual components using an appropriate mixing rule (e.g., Kay's rule or Prausnitz-Gunn method) [39].	$Z = 1 + \left(0.31506 - \frac{1.0467}{T_r} - \frac{0.5783}{T_r^3}\right)\rho_r +$ $(0.5353 - \frac{0.6127}{T_r} - \frac{0.6185}{T_r^3})\rho_r{}^2$Reduced density, $\rho_r = 0.27\left(\frac{P_r}{Z_i T_r}\right)$, as NG specific density	T_c = Critical Temperature (K) p_c = Critical Pressure (Pa) Z_i = Initial compressibility factor Reduced Temperature,$T_r = \frac{T}{T_c}$ Reduced Pressure,$P_r = \frac{p}{P_c}$	(7)
Gas density (m^3/kg)		$Density = \frac{PM}{ZRT}$		(8)
Average pipeline gas pressure (Pa)	Due to pressure drops along the pipeline, the gas pressure varies across different segments. To simplify calculations for a given pipeline section, an average pressure is used. This approach ensures consistent thermodynamic and flow analyses while accounting for the continuous pressure gradient.	$p = \left(\frac{2}{3}\right) \times \left[P_1 + P_2 - \frac{P_1 \times P_2}{P_1 + P_2}\right]$		(9)
Gas velocity (m/s)		$v = 14.7359 \times \left(\frac{q \times 24 \times 3600}{\left(D_0 \times 10^3 - 2 \times t \times 10^3\right)^2}\right) \times \left(\frac{P_b}{T_b}\right) \times \left(\frac{Z \times T}{P \times 10^2}\right)$	q = Gas flow rate (m^3/s) D_0 = Outer diameter of the pipeline (m) t = Pipe thickness (m) P_b = Base pressure (KPa) T_b = Base temperature (K)	(10)
Major constraints				
Maximum allowable operating pressure	To guarantee safe pipeline operation, the Maximum Allowable Operating Pressure (MAOP) must be carefully controlled to avoid structural damage. MAOP is calculated using equation (12) with wall thickness from equation (13), adhering to API 5L standards for pipe dimensions and materials. The Specified Minimum Yield Strength (SMYS) is set at 2000 bars, typical for high-strength steel pipelines. Safety factors, generally 0.72 for cross-country and offshore pipelines but varying to as low as 0.4 depending on location and construction type, are applied. The seam joint factor, ranging from 1 to 6, accounts for weld quality and material uniformity [19]. Temperature variations further influence MAOP through the temperature deration factor. For gas temperatures below 120 °C, $f_T = 1$; however, at elevated temperatures (≥230 °C), it decreases to 0.867 to compensate for the reduced material strength. These factors collectively ensure that the pipeline operates within safe mechanical limits, striking a balance between efficiency and long-term reliability.	$p < MAOPMAOP = SMYS^*\frac{2t}{D}^*f_F f_E f_T$Pipe Thickness,$t = 52 \times 10^{-3} D + 989 \times 10^{-7}$	SMYS = Specified minimum yield strength (2000 bar for ASME B36.19 M stainless steel) of pipe material f_F = Design factor (0.72) f_E= Seam joint factor (1.0) f_T = Temperature deration factor	(11) (12) (13)
Velocity of gas flow	The maximum velocity a compressible fluid can attain in a pipeline is known as the sonic (or critical) velocity. Exceeding this limit can lead to choked flow, causing operational instabilities and potential mechanical damage. To ensure safe and efficient pipeline operation, gas velocities are typically maintained below 50 % of the sonic velocity. The sonic velocity of a gas can be approximated using equation (15), which depends on the average isentropic exponent.	$v < c/2c = \sqrt{\frac{kZRT}{M}}$	c = Sonic velocity of gas (m/s)	(14) (15)
Erosional velocity	The velocity of gas flow in pipelines must be carefully regulated to maintain system integrity and operational efficiency. Excessive gas velocity can lead to increased turbulence, pressure fluctuations, and mechanical vibrations, resulting in higher noise levels and potential structural risks. These effects can accelerate impingement attack, erosion-corrosion, and cavitation, all of which compromise pipeline durability and safety. To mitigate these risks, pipeline design incorporates an upper velocity limit, which provides an empirical basis for determining safe flow speeds. Additionally, the erosional velocity, defined by equation (17), serves as a critical threshold. This value, which must always remain below the speed of sound in the pipeline, ensures	$v < v_e v_e = 122\sqrt{\frac{ZRT}{PM}}$	v_e = Erosional velocity (m/s)	(16) (17)

(*continued on next page*)

Table 2 (*continued*)

Equation Name	Description	Equation	Parameters	Eqn. no.
	that flow-induced wear does not exceed acceptable limits [1].			
Energy and economic-based equations				
Marginal abatement cost (MAC)	The MAC is an important matrix to evaluate the cost-effectiveness of emission reduction strategies [40].	$MAC = \frac{\Delta Annualemissionsreduction}{\Delta Annualcost}$		(18)
Energy return on investment	EROI measures usable energy output versus energy input; a higher EROI in gas pipelines means less energy is used for compression, thereby improving efficiency [41].	$EROI = \frac{Energy\ delivered}{Energy\ used\ for\ compression}$		(19)
Energy intensity ratio	Energy intensity ratio (EIR), as a simplified inverse of EROI, reflects the fraction of useful energy input per unit of output energy [42].	$EIR = \frac{1}{EROI}$		(20)

% *iso*-butane, 0.015 % n-butane, 0.004 % *iso*-pentane, 0.004 % n-pentane, 0.003 % n-hexane, 3.99 % nitrogen (N_2), and 0.20 % carbon dioxide (CO_2). This composition represents processed, pipeline-quality natural gas and was originally used for combustion and air-emissions modeling in the LNG Canada Air Quality Technical Data Report [43].

3.1. Model validation

Model validation is essential for NG transmission pipelines with H_2 injection to ensure the accuracy and reliability of simulation results under new operating conditions. H_2 alters the gas mixture's thermodynamic, flow, and material interaction properties, which can significantly impact pressure, flow rate, and pipeline integrity. Validating the model helps identify and correct discrepancies, increasing confidence in predictive performance. This process ensures safe, efficient, and regulation-compliant operation when H_2 is blended into the NG network. In this section, data from two published papers have been compared with data generated by the present model. Khan et al. [44] considered a pipeline of 1500 km for H_2 transportation and considered a compressor station every 500 km, 300 km, and 100 km distances. The schematic pipeline diagram for the three scenarios is shown in Fig. 6. The initial pressure to the initial compressor from the gas processing plant is 2 MPa, and the initial pressure to the first compressor is 7 MPa. The values used for the modeling are presented in Table 3. **Equation (21)** is used for the validation, considering an additional parameter for the elevation of the pipeline [6].

Fig. 7 illustrates the H_2 transportation capacity (t_{H_2}/day) of pipelines as a function of the nominal pipe size (NPS) for three different inter-compressor station distances. Specifically, Fig. 7(a) presents data extracted from a reference study, while Fig. 7(b) displays the results from the present study, which are based on the same input parameters for consistency and comparative analysis. In both figures, the H_2 capacity is evaluated for pipeline diameters of 10-inch, 14-inch, 18-inch, 24-inch, 36-inch, 42-inch, and 48-inch (corresponding to 0.25 m, 0.36 m, 0.46 m, 0.7 m, 0.91 m, 1.07 m, and 1.22 m, respectively) and for compressor station spacings of 100 km, 300 km, and 500 km. For simplification and computational efficiency, the present study approximates the pipe sizes as 10-inch, 20-inch, 30-inch, 40-inch, and 50-inch. Despite this approximation, the results of the present study exhibit trends and capacity values that closely align with those reported in the reference work. Minor deviations observed between the two datasets may be attributed to differences in the assumed molar mass of H_2 in the thermodynamic calculations, which can influence the flow capacity estimations.

Fig. 8 presents the outlet pipeline pressures (bar) for different pipe sizes, considering 500 km, 300 km, and 100 km compressor distances for the current study (b), and the reference study (a). The results of the current study show similar trends and values as in the reference study. From Fig. 8(a), the outlet pressures for pipe sizes 10-inch, 30-inch, and 30-inch are around 14 bar, 26.5 bar, and 32.5 bar, respectively, for a 500 km compressor distance, whereas in the present study, these are 14.4 bar, 26.9 bar, and 32.8 bar, correspondingly, as shown in Fig. 8(b). Similarly, the results are also close to the reference paper for 300 km and 100 km compressor distances.

The model developed in the current study is also validated against a study of an H_2 pipeline network [45]. In this study, the pipeline is simulated using Aspen Plus with an H_2 transmission pipeline and multiple enroute stations. The input station compresses the H_2 gas to the design pressure before it is released from the alkaline electrolyzer. Next, as depicted in Fig. 9, it is transported via the H_2 transmission pipelines. The simplified schematic diagram is depicted in Fig. 10 for a 4 MPa inlet pressure to the enroute stations, where five enroute stations are considered and the distance between two enroute compressor stations is 300 km.

The information used for this validation is presented in Table 4. The transmission distance is 1800 km for a gas transmission rate of 28.80 kg/s, considering a diameter range of 500 mm to 900 mm. The base pressure and molar mass are assumed in the present study, as it is not mentioned in the reference paper. The inlet pressure is 1.6 MPa, after which the pressure is raised to 4 MPa to 10 MPa by the inlet compressor. Then the gas flows into the transmission line and through the enroute stations. A compression ratio of 2.0 is considered in all cases.

Figs. 11(a) and (b) show the compressor power for each station (kW) (left vertical axis) and the number of enroute stations (right vertical axis) versus design pressure after compression of the inlet station for the reference paper and the present study. For design pressure 4 MPa, the compressor power for the inlet station and enroute stations are 3.98×10^4 kW and 2.10×10^5 kW, respectively, where the enroute station is composed of five compressors. Similarly, the compressor power for inlet station and enroute stations for 6 MPa, 8 MPa, and 10 MPa design pressures are 7.48×10^4 kW and 1.37×10^5 kW, 8.26×10^4 kW and 2.02×10^5 kW, 9.43×10^4 kW and 2.56×10^5 kW, respectively, considering 4, 5, and 6 enroute stations. All the results in the present study follow similar trends and are almost the same as the reference paper.

Fig. 12 shows the pipe nominal diameter corresponding to the annual gas transmission amount (Mtons/year) for 4 MPa, 6 MPa, 8 MPa, and 10 MPa inlet pressure in case of (a) the reference paper, and (b) the present study. The results obtained from the present study show similar trends and values to those in the reference paper. The small difference in the results is because of some difficulties in the study. The major difficulties were due to the lack of information about the pipeline length and the number of enroute stations in the transmission pipeline. Therefore, for the simplicity of the simulation single compressor is assumed, and a 300 km pipeline length is assumed. Table 5. shows the input parameters considered for the study.

4. Results and discussion

Fig. 13 illustrates the maximum operating pressure in the

Method	Key Features	Advantages	Limitations in Pipeline Context
Genetic Algorithm (GA)	Population-based, inspired by natural selection and uses crossover and mutation.	Handles nonlinear, non-convex, and discrete problems. But does not require gradient. Strong global search capability and flexible with multiple objectives.	Computationally intensive if population size/iterations are large.
Particle Swarm Optimization (PSO)	Swarm intelligence; particles update positions based on velocity and best-known solutions.	Fast convergence, good for continuous problems and simple implementation.	Prone to premature convergence, weaker constraint handling, sensitive to parameter tuning.
Ant Colony Optimization (ACO)	Probabilistic search inspired by ant foraging.	Effective for discrete routing and network optimization; good at combinatorial problems.	Less efficient in continuous multi-variable problems; high computational overhead in large networks.
Generalized Reduced Gradient (GRG)	Gradient-based, deterministic local search.	Fast for smooth, convex optimization; widely used in linear/nonlinear programming.	Requires differentiable objective; prone to local minima; unsuitable for highly nonlinear or discontinuous problems.

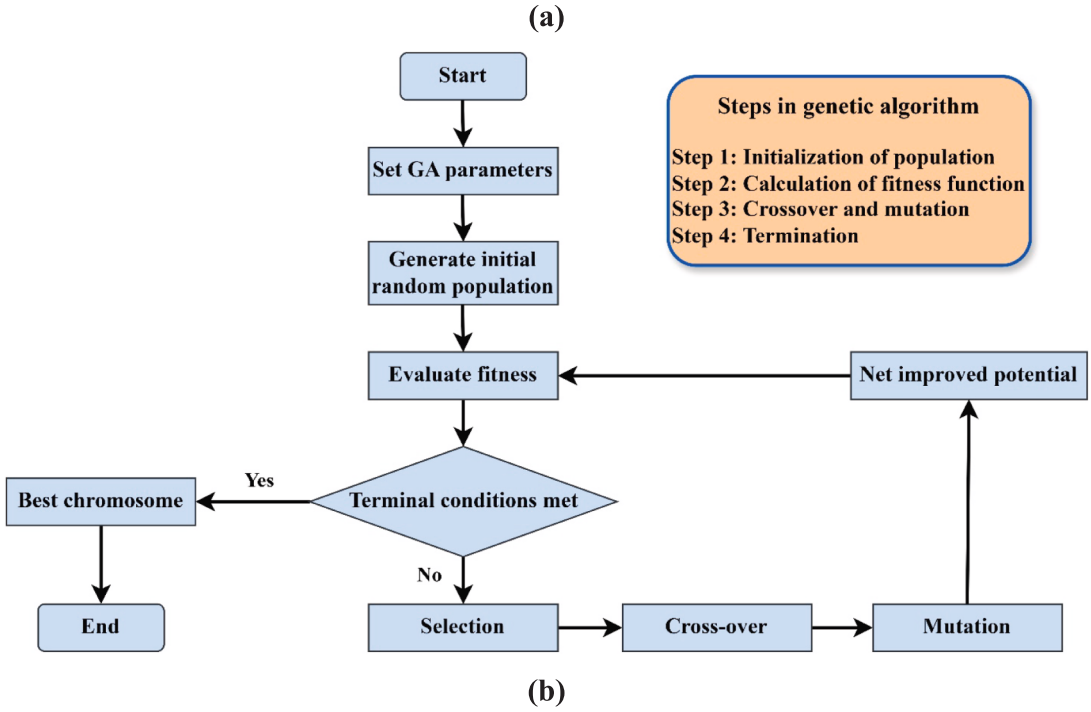

Fig. 3. (a) Comparative summary of optimization methods, (b) Genetic algorithm flow chart for natural gas pipeline optimization [6].

transmission pipeline for various transmission lengths, considering different gas compositions: 100 % NG, 10 % H_2, 20 % H_2, and 100 % H_2 (vol%). The 100 % NG and 100 % H_2 cases define the performance boundaries of pure natural gas and pure H_2 operation, whereas 10 % H_2 and 20 % H_2 blending ratios were selected because they align with thresholds highlighted in several national and regional H_2 strategies [45,48]. For instance, 10 % blending is often treated as a conservative entry point for pilot projects and grid injection trials, while 20 % represents an upper bound currently regarded as achievable within existing pipeline systems under appropriate regulatory approval. By analyzing these policy-relevant scenarios, the study provides insights that are directly applicable to infrastructure planning and decarbonization strategies currently under consideration by governments and industry [3]. The maximum operating pressure for a 100 km pipeline with a single compressor increases with higher H_2 content in the gas mixture, with 100 % H_2 showing the highest pressure, followed by 20 %

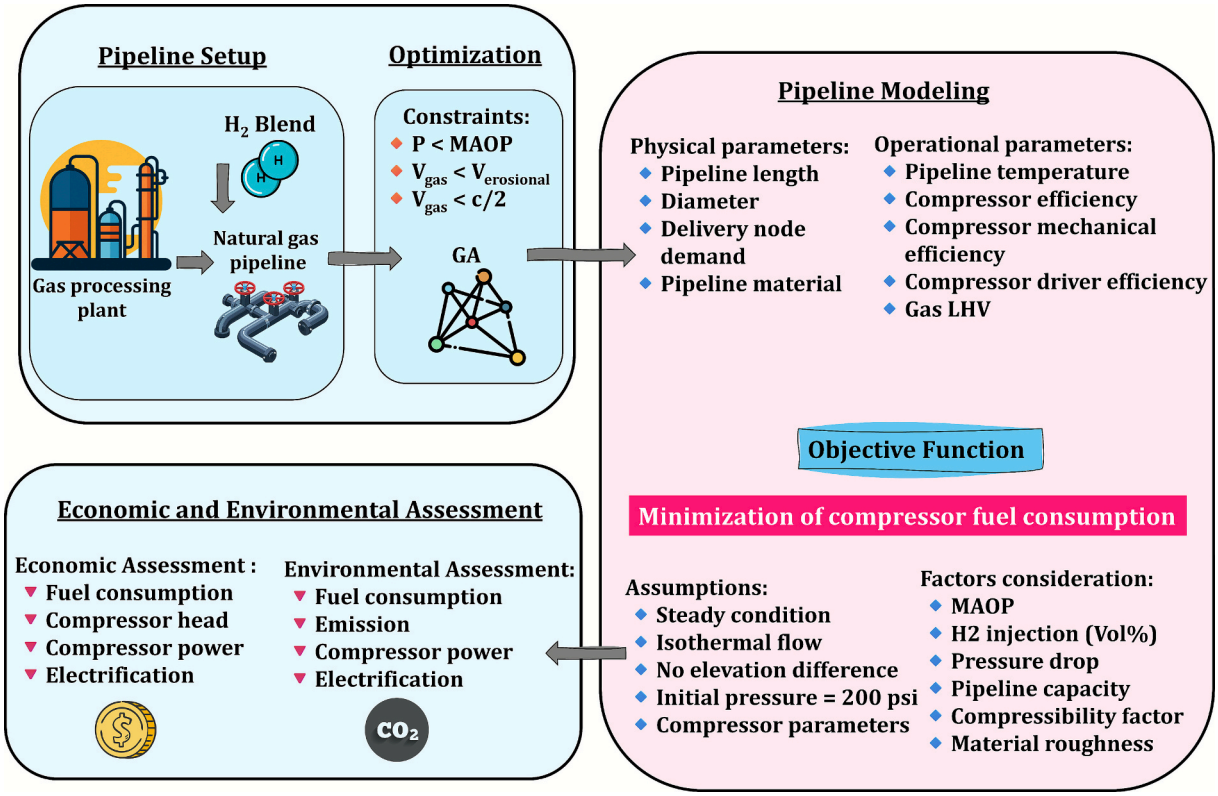

Fig. 4. Schematic illustration of the framework for the present study.

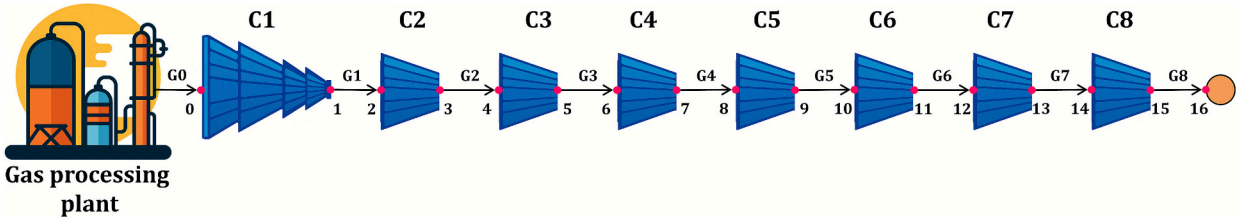

Fig. 5. Simple transmission line with single delivery point.

H_2, 10 % H_2, and 100 % NG.

As the pipeline length increases, the maximum operating pressure also rises, though the rate of increase diminishes for lengths exceeding 500 km compared to shorter pipelines. This indicates that longer pipelines experience less significant pressure growth. The trend suggests that the presence of H_2 in the gas mixture leads to a higher maximum operating pressure, with the highest pressure observed in pure H_2 pipelines. The minimum operating pressure for pipelines having a range of transmission lengths for different gas compositions is shown in Fig. 14. These figures show that the minimum pressure is obtained for 100 % H_2 transmission, followed by 20 % H_2, 10 % H_2 injection, and NG. The pressure drop of a gas with a lower molar mass tends to be higher due to several interconnected factors primarily governed by the principles of fluid dynamics and gas properties.

The pressure drop in a single pipeline increases with decreasing molar mass of the gas, meaning that NG experiences the lowest pressure drop compared to the other gas compositions. For all gas mixtures, the minimum operating pressure decreases as the transmission length increases. In longer transmission pipelines, the minimum operating pressure at the final node is higher for NG compared to the H_2-enriched mixtures. The presence of H_2 in the gas mixture results in progressively lower minimum operating pressures, with the lowest pressure observed for the pure H_2 composition.

Fig. 15 shows the fuel consumption percentage of the compressor relative to the total delivered fuel to the delivery node, considering a constant power delivery of 8 GW for three different gas compositions over varying pipeline lengths. The gas compositions include NG, a mixture of 10 % H_2 and 90 % NG (10 % H_2), and a mixture of 20 % H_2 and 80 % NG (20 % H_2). The NG fuel consumption line starts at about 1.42 % for 100 km and gradually increases to 2.98 % at 800 km. Moreover, the 10 % H_2-fuel consumption line starts slightly higher than NG at 1.6 % for 100 km and increases to about 3.73 % at 800 km. Furthermore, the 20 % H_2-fuel consumption line begins the highest among the three at around 1.85 % for 100 km and rises to approximately 4.43 % at 800 km.

For all pipeline lengths, the fuel consumption percentage increases with the amount of H_2 mixed with NG. The rate of increase in fuel consumption with pipeline length is higher for mixtures containing H_2 compared to pure NG. At longer distances, the difference in fuel consumption between the gas compositions becomes more pronounced. The higher the H_2 content, the greater the fuel consumption for the same pipeline length, indicating increased energy requirements for transmission.

Fig. 16 depicts the operating pressure (MPa) along an 800 km pipeline with eight compressors, corresponding to 16 pipeline nodes, for different gas compositions: NG, 10 % H_2, 20 % H_2, and 100 % H_2. The

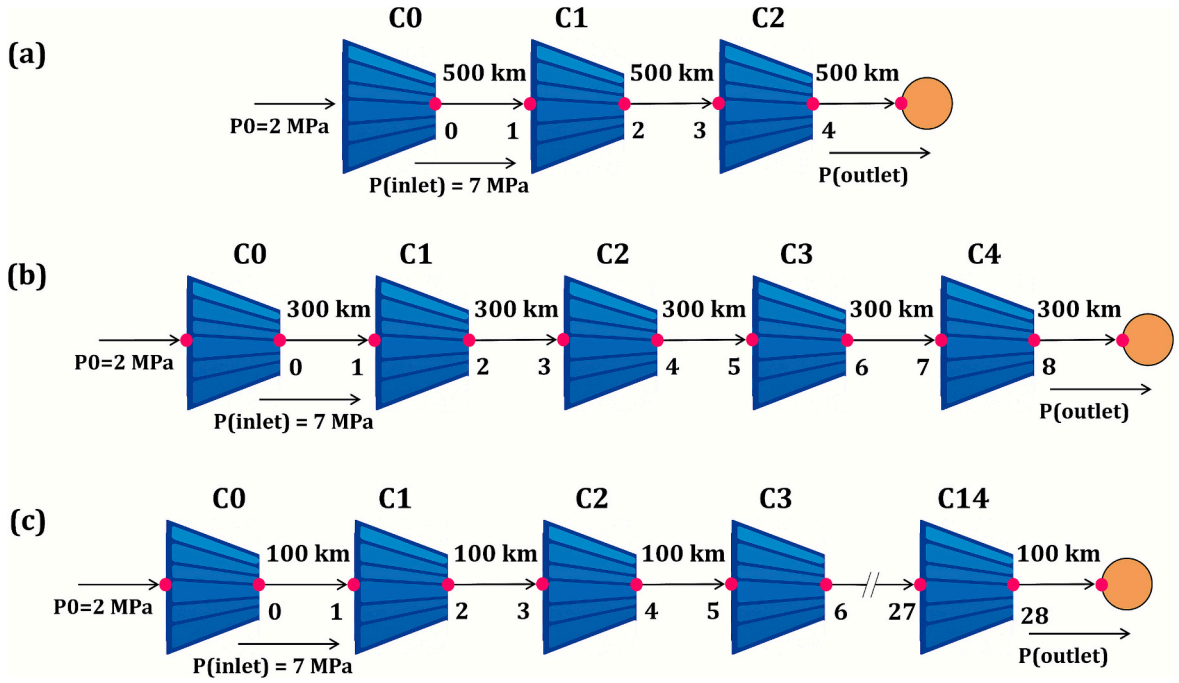

Fig. 6. 1500 km pipeline system for compressor distances of (a) 500 km, (b) 300 km, and (c) 100 km.

Table 3
Parameters and their values used in the validation [6].

Parameter	Value	Parameter	Value
Base pressure, P_b (kPa)	101	Compressor distance (km)	500, 300, and 100
Base temperature (K)	288.706	Pipe roughness (mm)	0.0178
Inlet pressure, P_1 (MPa)	7	Outlet gas velocity (m/s)	35
Full pipeline length (km)	1500	ni_{sen} (%)	80
Compression ratio	2.1	Z	1.031
H_2 gas density (kg/m^3)	0.08375	Molar mass, M (g/mol)	2.02 (assumed)
Elevation difference (m)	100		

delivery power for all the gases is 8 GW. The operating pressure generally decreases as the H_2 content increases in the gas mixture. Initially at the 1st node, the operating pressure is lowest for NG, and at the delivery end, it is maximum because of the lower pressure drop compared to other gases. The pressure fluctuations and drops become more pronounced with higher H_2 content, indicating a higher pressure drop along the pipeline for H_2-rich mixtures. In all cases, the minimum pressure follows the constraint of equal to or greater than 1.38 MPa (around 200 Psi).

The maximum delivered power (GW) and compressor fuel consumption (%) corresponding to variations in MAOP for three different gas compositions: NG, 20 % H_2, and 100 % H_2 are shown in Fig. 17. In the case of NG, delivered power remains consistently at 8 GW for MAOP values from 8.6 MPa to 5 MPa. Delivered power then decreases by decreasing MAOP and is 2.6 GW at 2 MPa. Like NG, delivered power for a 20 % H_2 gas mixture is 8 GW up to 5 MPa MAOP and decreases to 2.2 GW at 2 MPa. In the case of 100 % H_2, delivered power is 8 GW for higher MAOP (8.6 MPa to 6 MPa) but drops below 8 GW as MAOP decreases, dropping to about 1.6 GW for an MAOP of 2 MPa.

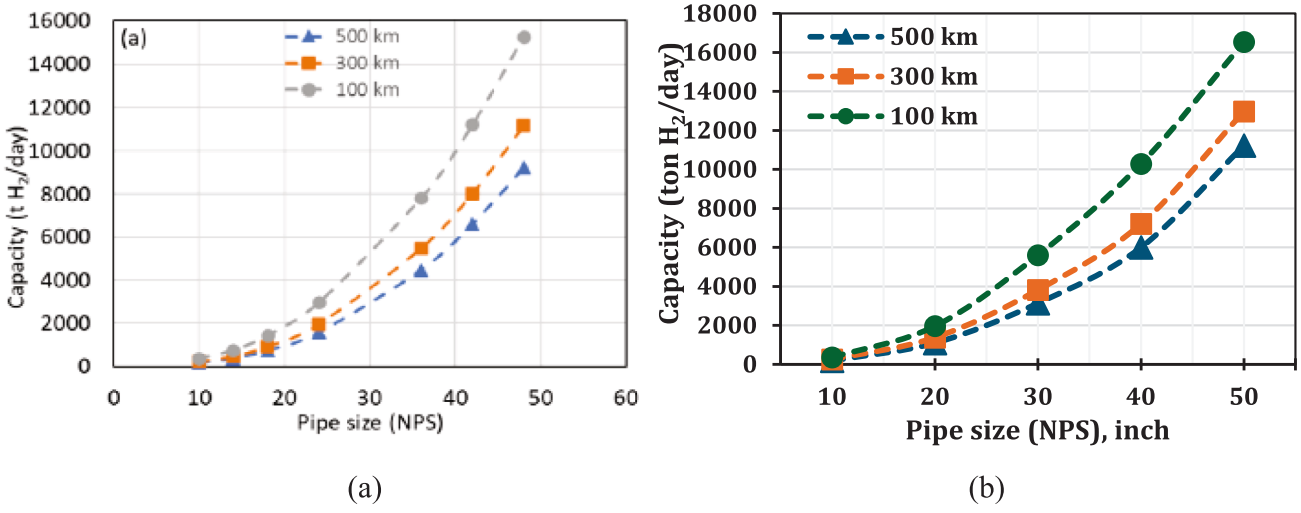

Fig. 7. Pipeline H_2 capacity (t_{H_2}/day) versus pipe size (NPS) as a function of distance between compressor stations for (a) reference paper, and (b) present study.

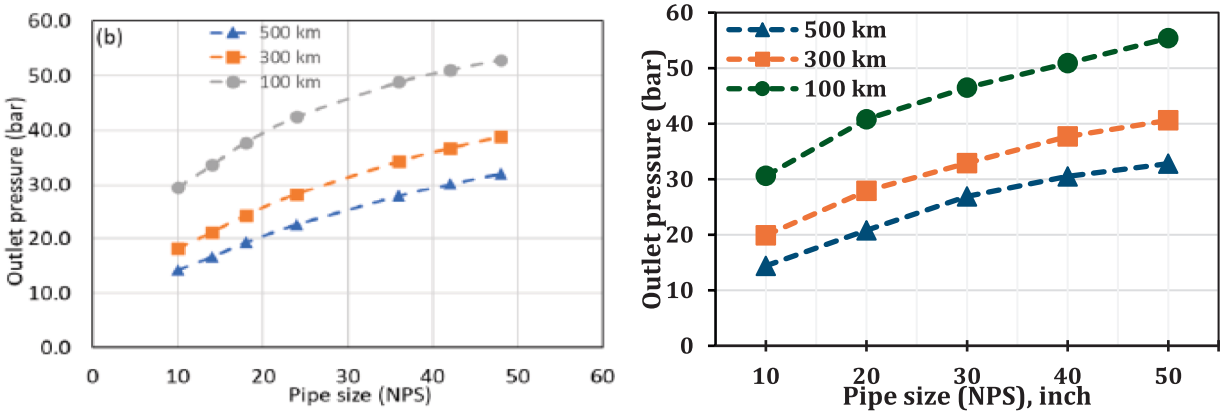

Fig. 8. Pipeline outlet pressure (bar) versus nominal pipe size (inch) as a function of compressor station distance for (a) reference paper, and (b) present study.

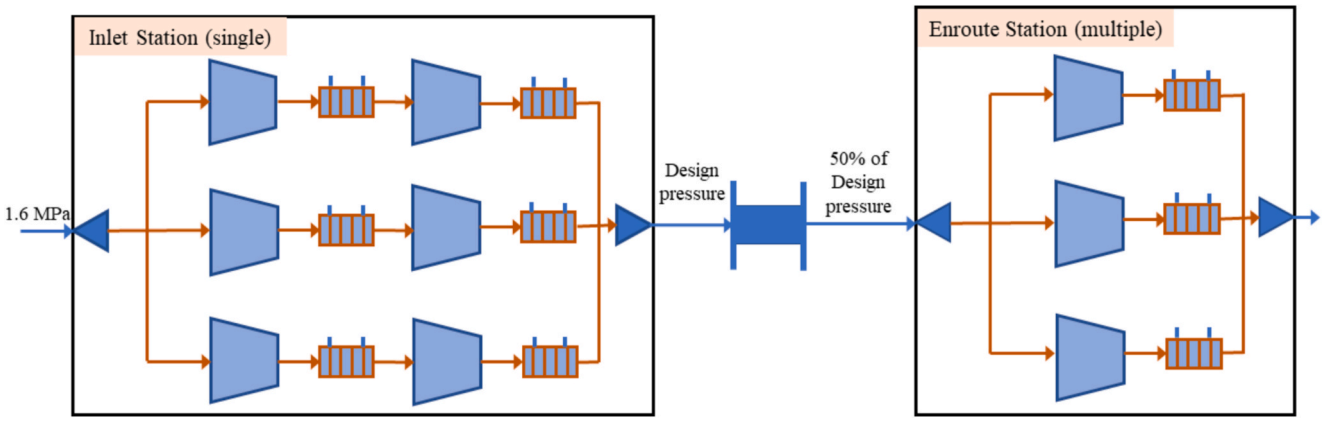

Fig. 9. Diagrammatic representation of the Aspen Plus process model from the reference paper [45].

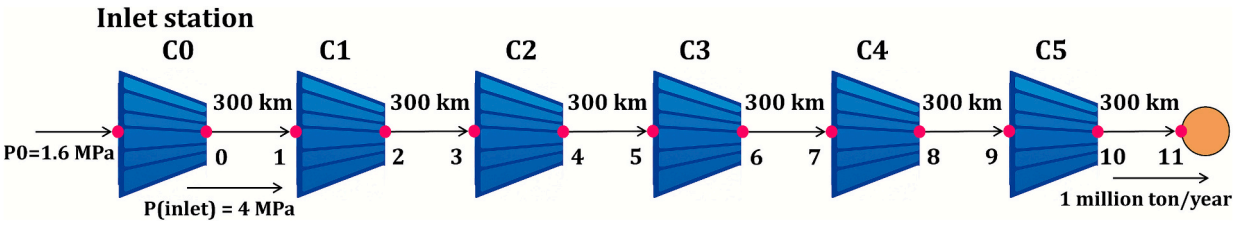

Fig. 10. Simplified schematic diagram of the considered model. The initial pressure is 1.6 MPa from the electrolyzer, and the inlet pressure to the enroute stations is 4 MPa to 10 MPa.

Table 4
Information used for the validation of the Yu et al. [45] reference paper.

Parameter	Value	Parameter	Value
Base pressure, P_b (kPa)	101.352 (assumed)	Nominal diameter (DN) (mm)	500 to 900
Base temperature (K)	293.15	n_i	0.8
Transmission distance (km)	1800	Mechanical efficiency	0.96
Molar mass, M (g/mol)	2.02 (assumed)	Gas flow rate (million ton/year)	1
Compression ratio	2	Gas flow rate (kg/s)	28.80
Pipe roughness (mm)	0.04		

Fuel consumption increases as MAOP decreases for all gas compositions with the same delivered power. However, the rate of increase is much steeper for 100 % H_2 compared to NG and 20 % H_2. From the figure, fuel consumption (%) increases gradually from 8.6 MPa to 5 MPa of MAOP whenever the delivered power is 8 GW, and the fuel consumption for a 20 % H_2 gas mixture is always higher than NG for all values of MAOP. After 5 MAOP, the fuel consumption decreases with the decreasing MAOP as the delivered power also decreases. The minimum fuel consumption for NG and 20 % H_2 is 2.96 % and 4.3 % at an MAOP of 2 MPa, where the delivered power is 2.6 GW and 2.2 GW. Fuel consumption is maximum (21.4 %) at 6 MPa, and then it gradually decreases to 14.6 % for 2 MPa. Overall, the fuel consumption gradually increases with the decreasing MAOP for delivering constant power. Moreover, if the delivered power decreases, then the fuel consumption also decreases with decreasing MAOP. Transitioning to H_2-rich mixtures requires careful consideration of MAOP to balance delivered power and fuel consumption, potentially requiring infrastructure upgrades to handle higher fuel consumption and maintain efficiency.

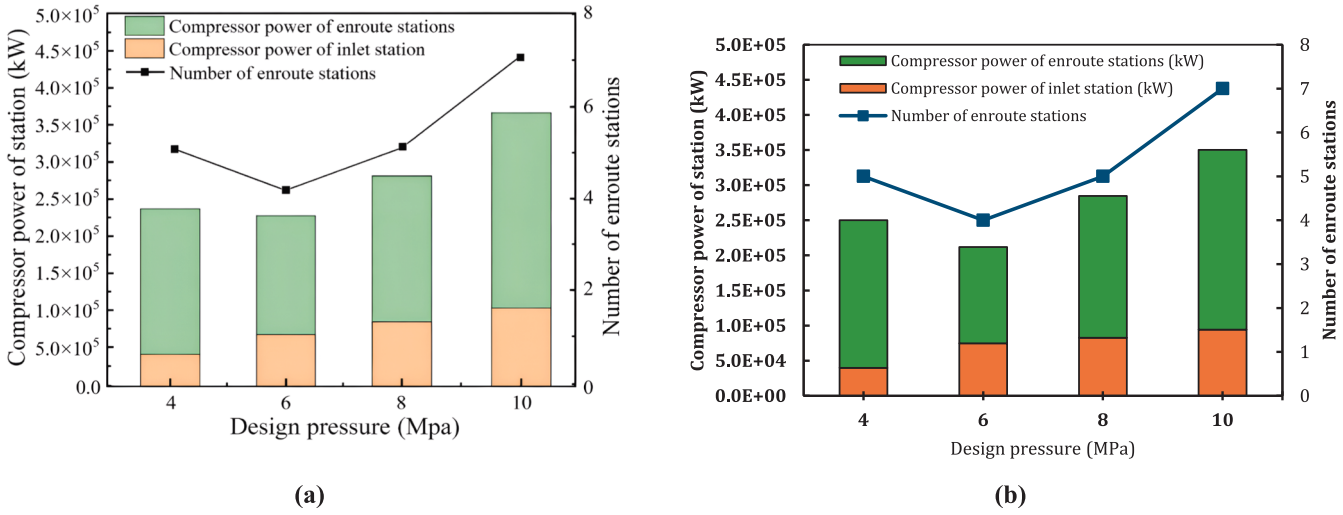

Fig. 11. Compressor power station (kW) and number of enroute stations versus design pressure (MPa) for (a) reference paper, and (b) present study.

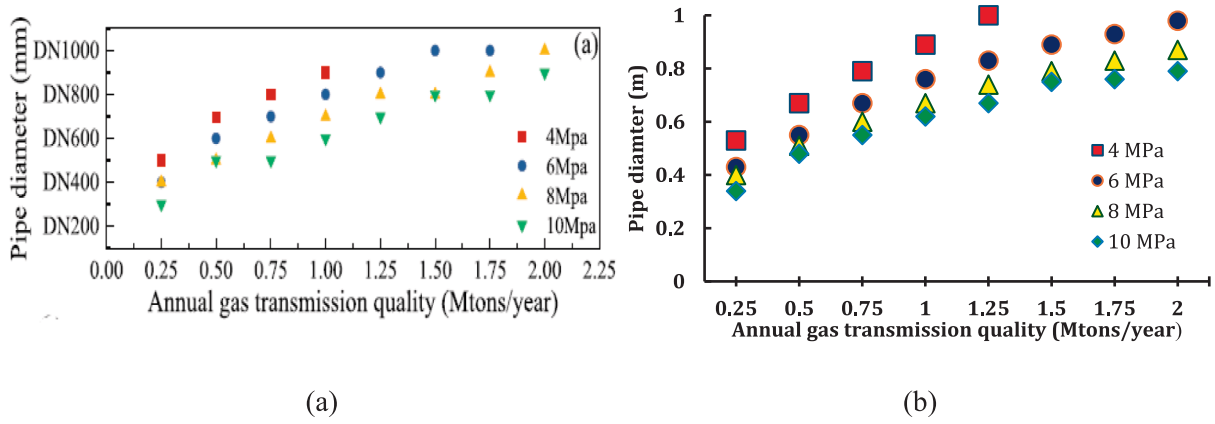

Fig. 12. Pipe nominal diameter corresponding with the annual gas transmission amount (Mtons/year) for 4 MPa, 6 MPa, 8 MPa, and 10 MPa inlet pressure in case of (a) reference paper, and (b) present study.

Table 5
Input parameters considered for the study.

Parameter	Value	Parameter	Value
Pipeline gas temperature, T (K)	283	Molar mass of NG (g/mol)	16.5
Universal gas constant, R (J/mol.K)	8.314	Molar mass of H_2 (g/mol)	2.02
Isentropic exponent, k	1.3	Lower heating value of NG (MJ/kg)	48.83
Compressor isentropic efficiency	0.72	Lower heating value of H_2 (MJ/kg)	120
Compressor mechanical efficiency	0.9	Critical temperature of NG (K)	190.9
Compressor driver efficiency	0.35	Critical temperature of H_2 (K)	33.2
Steel pipe roughness, ε (μm)	50	Critical pressure of NG (Pa)	4.58×10^6
Density of NG at standard conditions (kg/m^3)	0.712	Critical pressure of H_2 (Pa)	1.31×10^6
Density of H_2 at standard conditions (kg/m^3)	0.0898	Initial gas pressure to 1st compressor (MPa)	1.38

5. Case Study: Coastal GasLink pipeline Ltd

An existing NG transmission pipeline is optimized in the present study. Coastal GasLink Pipeline Ltd. is at the forefront of a significant energy infrastructure project aimed at transporting NG from north-eastern British Columbia to the LNG Canada export facility in Kitimat, BC, as shown in Fig. 18. The pipeline spans approximately 670 km and features a substantial diameter of 1.219 m. Designed to meet a variable daily demand ranging from 56 to 85 million cubic meters, the project underscores the need for efficient and scalable NG transportation. To maintain optimal flow and pressure across this extensive network, the pipeline will incorporate up to eight compressor stations strategically located along the route. This infrastructure not only enhances energy export capabilities but also plays a pivotal role in supporting economic growth and energy security in the region, making it an intriguing case for optimization modeling and analysis.

The Coastal GasLink Pipeline Ltd. system is introduced as a real-world case study to evaluate the applicability of the proposed optimization framework under practical design, operational, and demand conditions. Unlike the simplified system shown in Fig. 5, this case study incorporates project-specific pipeline length, diameter, demand variability, and compressor station configuration.

5.1. Effect of maximum allowable operating pressure

Fig. 19 illustrates the relationship between the MAOP and two key performance metrics: the delivered mass flow rate (measured in kg/s) and fuel consumption (measured in percentage) for the Coastal GasLink

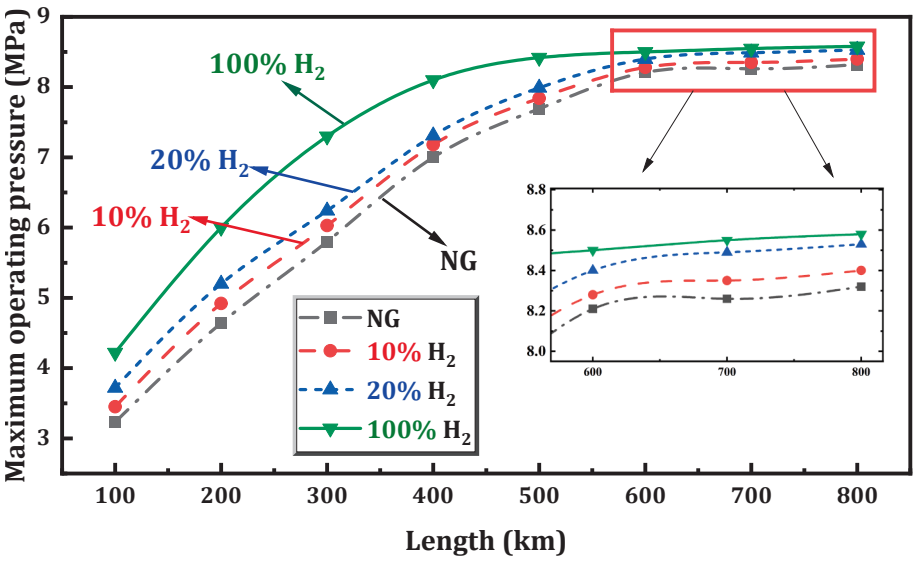

Fig. 13. Maximum operating pressure (MPa) in the transmission pipeline for different pipeline lengths (km).

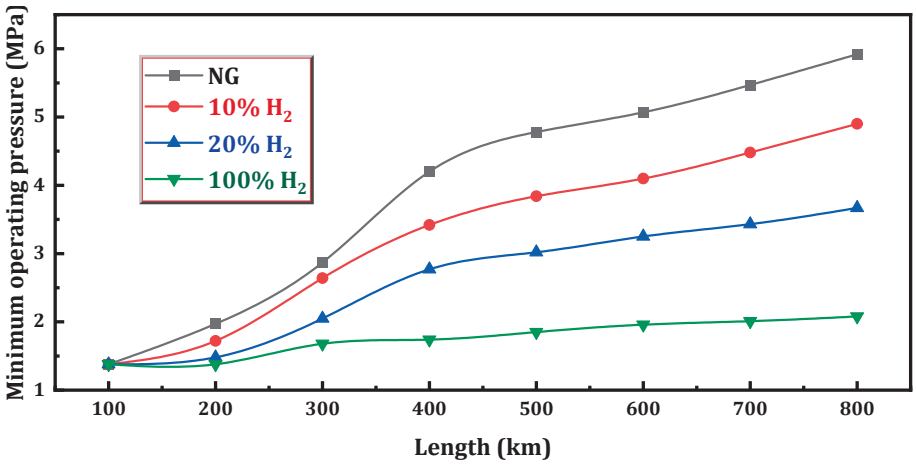

Fig. 14. Lower operating pressure (MPa) versus single delivery pipeline transmission length for different gas compositions.

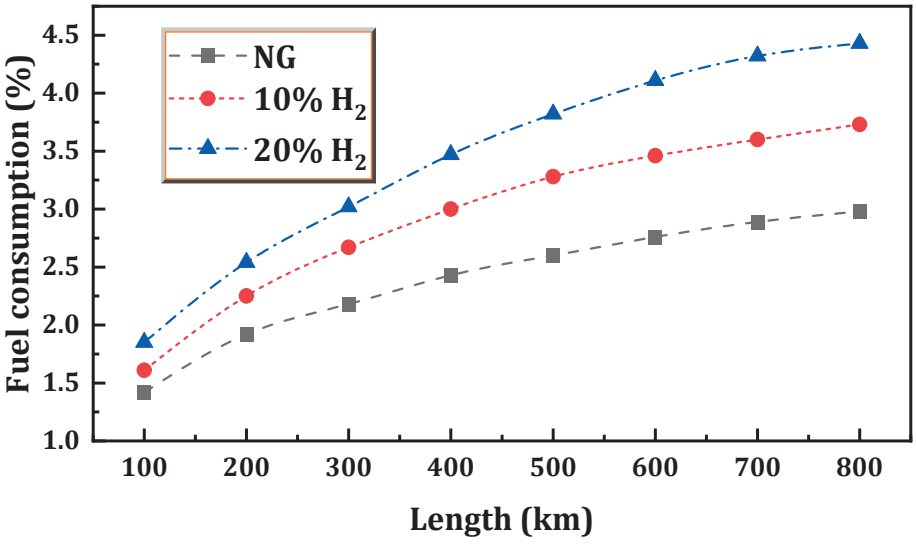

Fig. 15. Fuel consumption (%) variation at different pipeline transmission lengths (km) for different gas compositions to deliver 8 GW power.

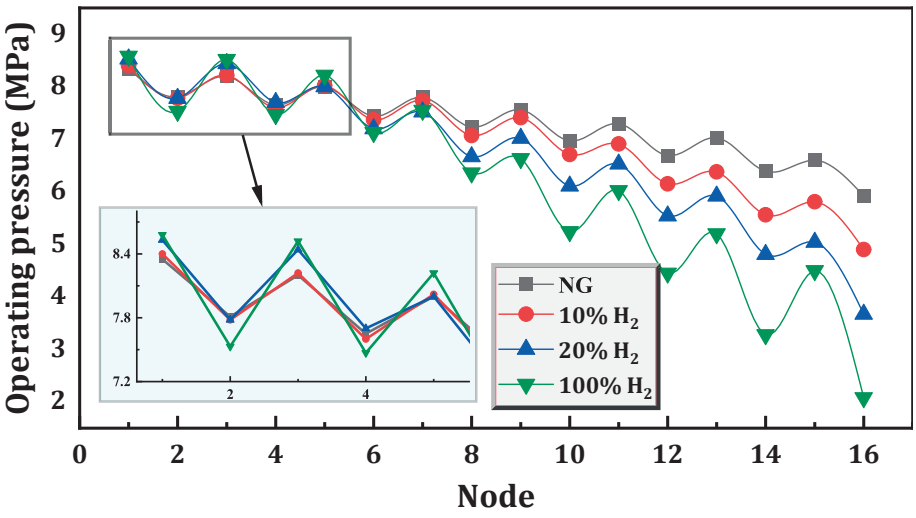

Fig. 16. Operating pressure (MPa) of the pipeline throughout at different nodes to deliver 8 GW power to a single delivery point.

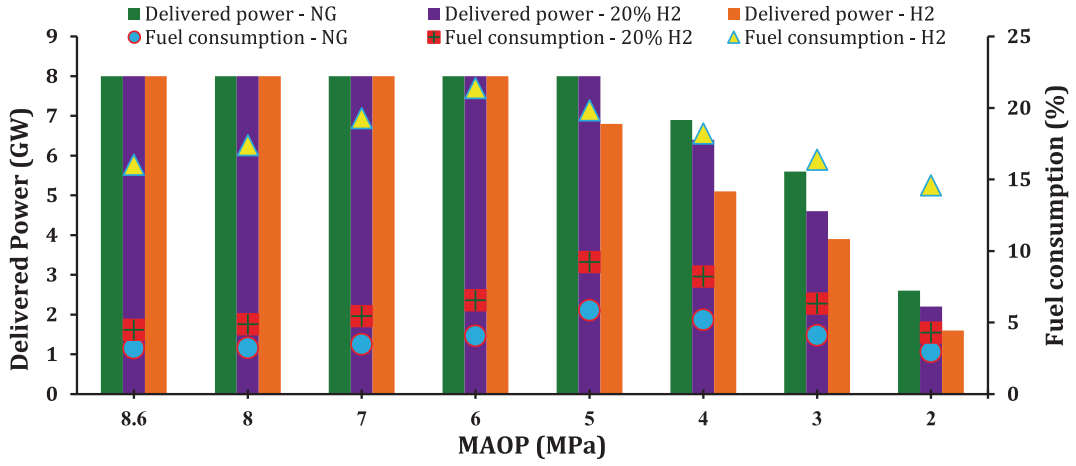

Fig. 17. Maximum delivered power (GW) and fuel consumption (%) corresponding to MAOP (MPa) variations for NG, 20% H_2 (vol%), and 100% H_2 gases.

Pipeline Ltd. case study. The MAOP values, ranging from 2 MPa to 8.2 MPa, are plotted along the x-axis, while the delivered mass flow rate is represented on the left y-axis, and fuel consumption is shown by the red line on the right y-axis.

As MAOP decreases from 8.2 MPa to 2 MPa, the delivered mass flow rate initially shows a constant value of 431.3 kg/s until 4 MPa, beyond which it is not possible to supply the same mass flow rate because of the low-pressure boundary constraint ($p \geq 1.38$ MPa). This indicates that higher pressures enable a greater volume of NG to be transported through the pipeline, maximizing its delivery capacity. On the other hand, fuel consumption exhibits a different trend: it starts low, rises sharply to a peak (8.97 %) around 4 MPa, and then gradually decreases as MAOP continues to decrease. Overall, fuel consumption increases with an increase in MAOP for the same mass transfer capacity, but it decreases with a decrease in capacity, even when MAOP is low. The interplay between these factors highlights the importance of optimizing MAOP to balance high mass flow rates with acceptable fuel consumption levels, ensuring both economic and operational efficiency in pipeline management.

Electrifying compressor stations in NG transmission systems offers numerous benefits, primarily through reducing emissions, enhancing energy efficiency, and improving operational reliability. By replacing gas turbines with electric motors, companies can significantly lower CO_2 emissions, especially when powered by renewable energy, which helps meet environmental regulations and sustainability goals. Electric motors are also more energy-efficient, require less maintenance, and provide greater flexibility in managing gas flow and pressure, leading to more reliable operations.

5.2. *Electrification for GasLink pipeline*

Fig. 20 presents a comparative analysis of emissions and compressor power supply costs associated with four distinct energy configuration scenarios for the Coastal GasLink Pipeline Ltd. In this case, all the parameters considered are stated in Table 6. The figure underscores the trade-offs between environmental and economic factors inherent in the selection of compressor fuel sources. In Case 1, wherein all compressor stations are powered exclusively by NG, the system exhibits the highest annual CO_2 emissions from fuel combustion, amounting to approximately 1570 $ktCO_2$. Despite the elevated emissions, this configuration incurs the lowest annual compressor power supply cost, estimated at 56 M$/year, indicating economic favorability at the expense of environmental performance.

Conversely, Case 2 introduces a hybrid configuration in which the first compressor operates on NG, while the remaining compressor stations are powered by electricity. This transition significantly reduces the associated emissions to approximately 1066 $ktCO_2$ per year, reflecting improved environmental performance. However, this benefit is offset by

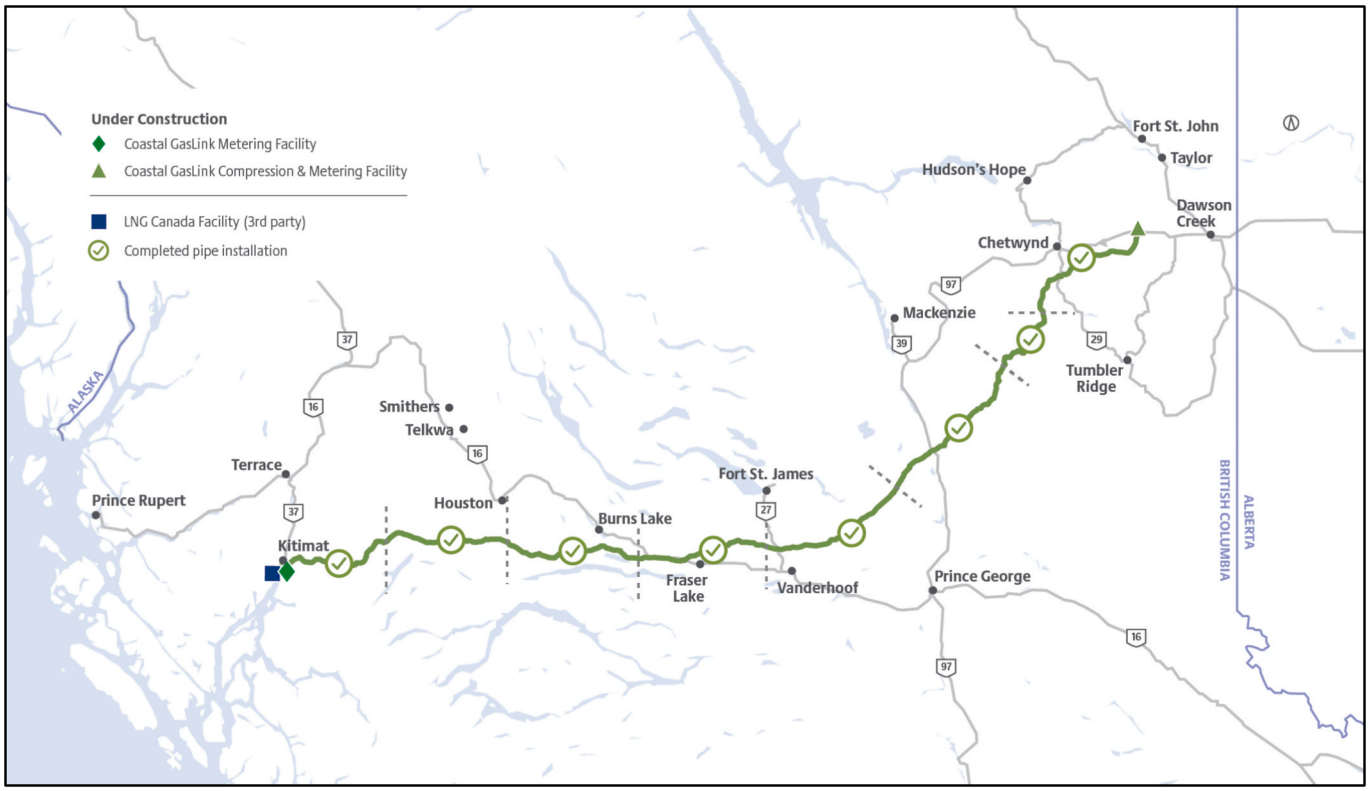

Fig. 18. Coastal GasLink transmission pipeline in Canada [46].

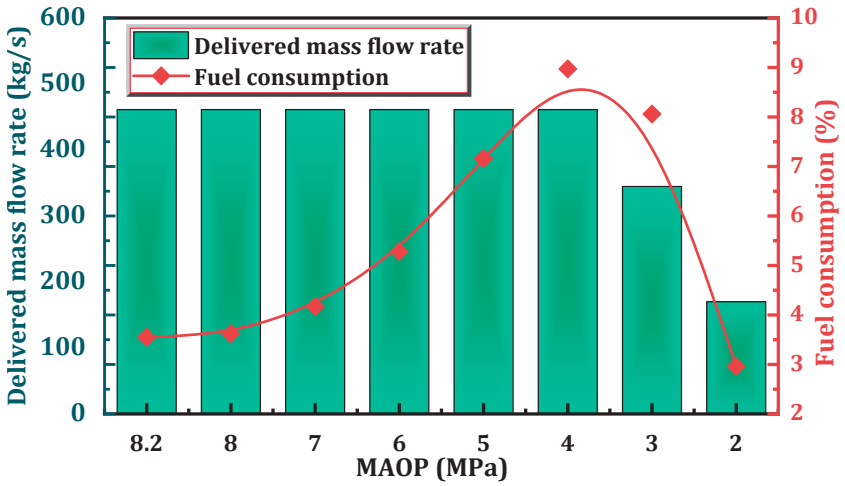

Fig. 19. Effect of MAOP on the delivered mass flow rate (kg/s) and fuel consumption (%) in a case study of Coastal GasLink Pipeline Ltd.

a substantial increase in operational expenditure, with the total compressor power supply cost rising to approximately 262 M$/year. This marked increase in cost is primarily attributed to the higher price of electricity relative to NG and the associated infrastructure requirements for electrification. These findings highlight the critical balance between environmental impact mitigation and economic feasibility when optimizing compressor energy configurations in large-scale NG transmission systems.

In Case 3, the energy configuration is partially electrified, with the first compressor station utilizing electricity, while the remaining compressor units continue to operate on NG. This configuration results in a further decline in total greenhouse gas emissions, reaching approximately 620 $ktCO_2$ per year, demonstrating a substantial improvement in emissions reduction relative to Cases 1 and 2. However, the corresponding compressor power supply cost increases significantly, reaching approximately 444 M$/year. The sharp rise in cost is largely attributable to the introduction of electrical infrastructure and the continued reliance on NG for the majority of compressors, which limits the full realization of operational cost savings from electrification.

Case 4 represents a fully electrified scenario, wherein all compressor stations are powered by electricity. This configuration achieves the lowest level of annual emissions, estimated at approximately 116 $ktCO_2$ per year, reflecting a near-complete mitigation of combustion-related carbon emissions. However, this environmentally optimal setup also imposes the highest annual compressor power supply cost, approximately 650 M$/year, due to the significant capital and operational expenditures associated with full-scale electrification and the higher cost of grid electricity compared to NG. Overall, although electrification of

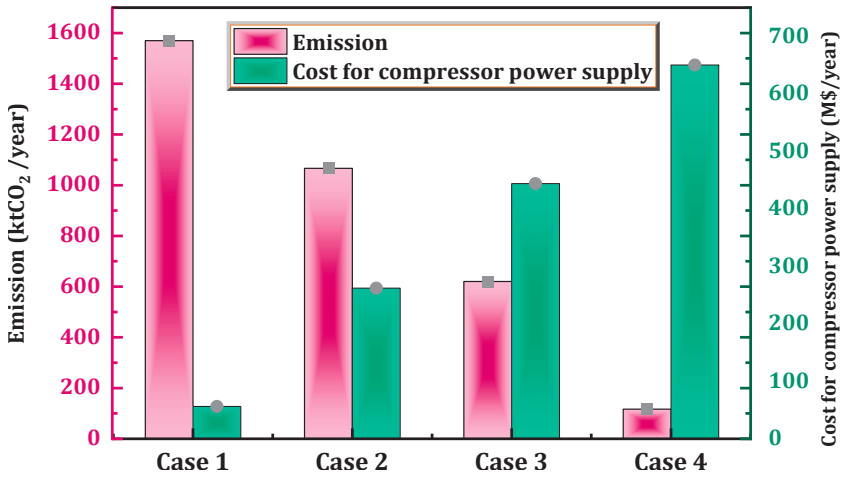

Fig. 20. Emission ($ktCO_2$/year) and cost for compressor power supply (M$/year) for different electrification levels.

Table 6
Parameters considered for electrification effect on the cost and emissions [47,48].

Parameter	Value	Parameter	Value
Motor efficiency	0.9	BC emission factor, kg CO_2/m^3	2.162
BC Electricity cost, $/kWh	0.0835	Density of NG, kg/m^3	0.712
Operating hours, hr./ year	8,760	Emission intensity, kg CO_2/kg NG	3.04
NG price, $/GJ	2.23	BC electricity emission factor, gCO_2e/kWh	15

compressors delivers low emissions, it requires more cost than a conventional NG-fueled turbine-compressor system. The figure highlights the trade-off between reducing emissions through increased electrification of compressors and the associated rise in power supply costs.

5.3. Comparison with Canada's 2030 emissions targets

Canada's official 2030 climate goal, as outlined in the 2030 Emissions Reduction Plan, is to reduce national GHG emissions by 40 %–45 % below 2005 levels, which equates to a national cap of approximately 402 $MtCO_2e$/year – 438 $MtCO_2e$/year by 2030 (from a 2005 baseline of ~ 730 $MtCO_2e$). The complete compressor station electrification along a single major transmission pipeline can contribute nearly 0.4 % of Canada's total emissions reduction requirement for 2030. While seemingly modest in percentage terms, this is a significant contribution from a single infrastructure project, especially given the scale and decentralized nature of Canada's emissions sources. Moreover, when viewed on a per capita basis, this is a meaningful reduction relative to the national per capita GHG emissions of ~ 17.5 tCO_2e/year, highlighting the potential of targeted infrastructure decarbonization projects to achieve incremental material progress toward national climate targets. Additionally, aligning such projects with Canada's broader H_2 and clean electricity strategies, such as the Clean Electricity Regulations, the Clean Fuel Regulations (CFR), and the H_2 Strategy for Canada, can amplify their systemic value.

5.4. Cost analysis

The cost-effectiveness of emission reduction strategies can be assessed using the MACC. The MACC framework is employed in this study to evaluate the economic trade-offs of electrifying compressor stations along an NG transmission pipeline in Canada, with a particular emphasis on the Coastal GasLink pipeline case. Several simplifying assumptions are made to compute the MAC for compressor station electrification. The analysis focused exclusively on operating costs, excluding capital expenditure and discounts, to reflect a steady-state, annualized perspective. The only direct CO_2 emissions that are taken into account are those from NG-fueled compressor combustion. The baseline configuration (Case 1) powered all compressors using NG, resulting in the highest annual CO_2 emissions, approximately 1570 $ktCO_2$ per year, at the lowest operational cost of approximately M $116.73. In contrast, a fully electrified configuration (Case 4) reduced emissions drastically to 56.22 $ktCO_2$ per year but increased the annual operating cost to M$650.16. The difference in emissions abatement between these two configurations amounts to 1513.45 $ktCO_2$/year, and the associated incremental cost is M$533.43/year (Fig. 21).

In the Canadian subsidy scenario, electricity costs are reduced by approximately 30 %–40 %, reflecting industrial or CleanBC-supported rates, leading to a lower MAC for the same emissions reduction. The MACC is constructed in incremental steps (e.g., 200, 400, 800, up to 1513.45 $ktCO_2$/year) assuming constant 8 GW power delivery and a uniform pipeline configuration. Without subsidy, the marginal abatement cost of full compressor station electrification reaches approximately $352 per tonne of CO_2. This reflects the high operational cost of replacing NG with grid electricity in the absence of financial incentives. However, when Canadian-style subsidies such as low-carbon electricity rates or CleanBC support are applied, the cost curve shifts downward

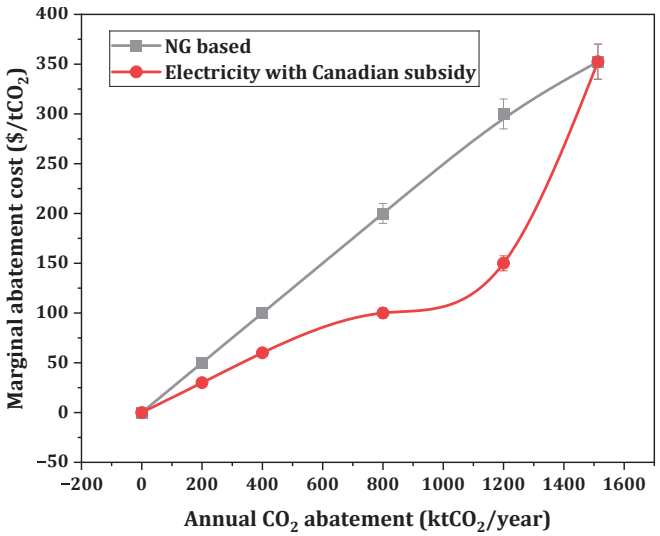

Fig. 21. Variation of marginal abatement with respect to CO_2 abatement.

significantly. As a result, electrification becomes a more economically viable strategy for emissions reduction in NG transmission systems.

5.5. Energy return on investment and energy intensity ratio analysis

The techno-economic and emissions study of compressor electrification and H_2 mixing is supplemented by an EROI and EIR assessment. The energy performance of the gas transmission system is measured in this analysis under various H_2 blending scenarios, with an emphasis on the energy given through the pipeline versus the energy used in compression. The EROI declines with increasing H_2 content in the pipeline, reflecting higher energy input requirements due to lower density of H_2 and higher compressibility. For 100 % NG, the system operates very efficiently, with an EROI of 33.56, meaning less than 3 % of the delivered energy is used for compression. The EROI drops to 22.57 with 20 % H_2 blending, suggesting increased compression loads and decreased energy efficiency. Because H_2 has a low molar mass and a large volumetric flow demand, the EROI for pure H_2 falls dramatically to 4.67, meaning that more than 21 % of the energy given is used in compression, as shown in Fig. 22.

The results presented in Fig. 22 indicate a clear increasing trend in the EIR with higher H_2 blending in natural gas pipeline transport. For the base case of 100 % NG, the EIR is 2.98, signifying relatively efficient transport with comparatively low energy expenditure per unit of energy delivered. However, when H_2 is introduced, the EIR progressively increases: 3.73 at 10 % H_2, 4.43 at 20 % H_2, and a substantially higher value of 21.4 for pure H_2 transport. This escalation reflects the higher energy requirements for compressing H_2 due to its lower volumetric energy density and distinct physical properties, such as lower molecular weight and higher compressibility. The sharp increase in EIR at 100 % H_2 highlights a critical challenge for pipeline decarbonization strategies, as the energy penalty associated with H_2 transport can significantly reduce the net energy available to end users. Thus, while moderate H_2 blending may be technically feasible, the substantial rise in EIR at higher H_2 fractions underscores the need for efficiency improvements, advanced compression technologies, or alternative transport methods to ensure the overall sustainability and viability of H_2 integration in pipeline systems.

6. Limitations and future research directions

British Columbia, Canada, holds significant renewable energy potential, with hydroelectricity supplying over 90 % of its power and wind capacity projected to grow to 3,500 MW by 2030 [49]. Canada's national H_2 strategy aims to supply 30 % of the country's end-use energy with clean H_2 by 2050, aligning with British Columbia's CleanBC goals to reduce emissions 40 % below 2007 levels by 2030 [50]. Blending H_2 into NG pipelines at concentrations up to 20 % could cut emissions by 6–7 % per year in BC, leveraging existing infrastructure while supporting decarbonization [1,26]. The province's abundant renewable resources position it as a key player in Canada's H_2 economy, with pilot projects already testing H_2-NG blends for grid injection. This integration supports both provincial and federal climate targets while advancing a low-carbon energy transition [51].

The schematic in Fig. 23 **(a)** presents a novel and integrated framework for the electrification of NG pipeline compressor stations using renewable energy sources, while simultaneously incorporating green H_2 production to enhance decarbonization. This hybrid energy system is designed to reduce reliance on fossil fuels by leveraging distributed renewable energy technologies, thereby minimizing greenhouse gas emissions and contributing to a cleaner gas transmission network. The electricity production subsystem consists of a mix of wind turbines, photovoltaic modules, and a diesel generator to ensure system reliability and energy resilience. These energy sources are coupled through a converter, which regulates power flow, and a battery storage system, which stabilizes intermittent renewable output and supports load balancing. A dump load is incorporated to manage excess energy and maintain system integrity. Electricity generated from this hybrid system is utilized in two primary pathways. First, it powers NG compressor stations, enabling compressor electrification. Electrifying compressors with renewable electricity significantly reduces direct CO_2 emissions from combustion-based compression processes.

Secondly, the renewable electricity is supplied to an electrolyzer, which uses water as a feedstock to produce H_2 and O_2 via water electrolysis. The produced oxygen is separated for potential utilization or safe release, while the H_2 is injected into the NG stream at downstream compressor stations, creating an H_2-NG blend. The dual functionality of this framework simultaneously compressor electrification and H_2 production, marking a significant step toward sector coupling and energy system decarbonization. It enables the use of surplus renewable energy for H_2 generation, thereby enhancing system efficiency and supporting grid stability. Furthermore, the modular nature of the setup allows scalability across different pipeline segments and geographical locations, adapting to local renewable resource availability. The integration of this framework aligns with Canada's national H_2 strategy and CleanBC climate goals.

The assumptions adopted in this study were necessary to ensure computational tractability and focus on system-level insights, but they inevitably simplify some real-world complexities. These limitations open up scopes for future research to refine and extend the present

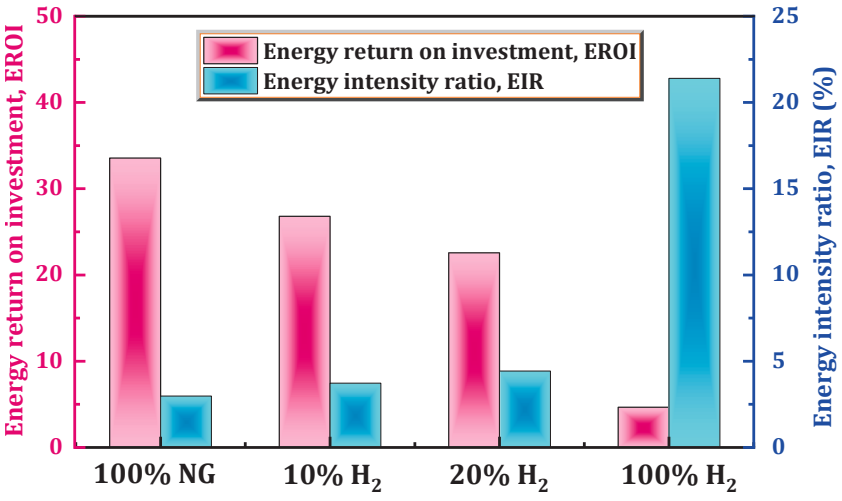

Fig. 22. Variation of EROI and EIR with respect to different percentages of H_2 injection.

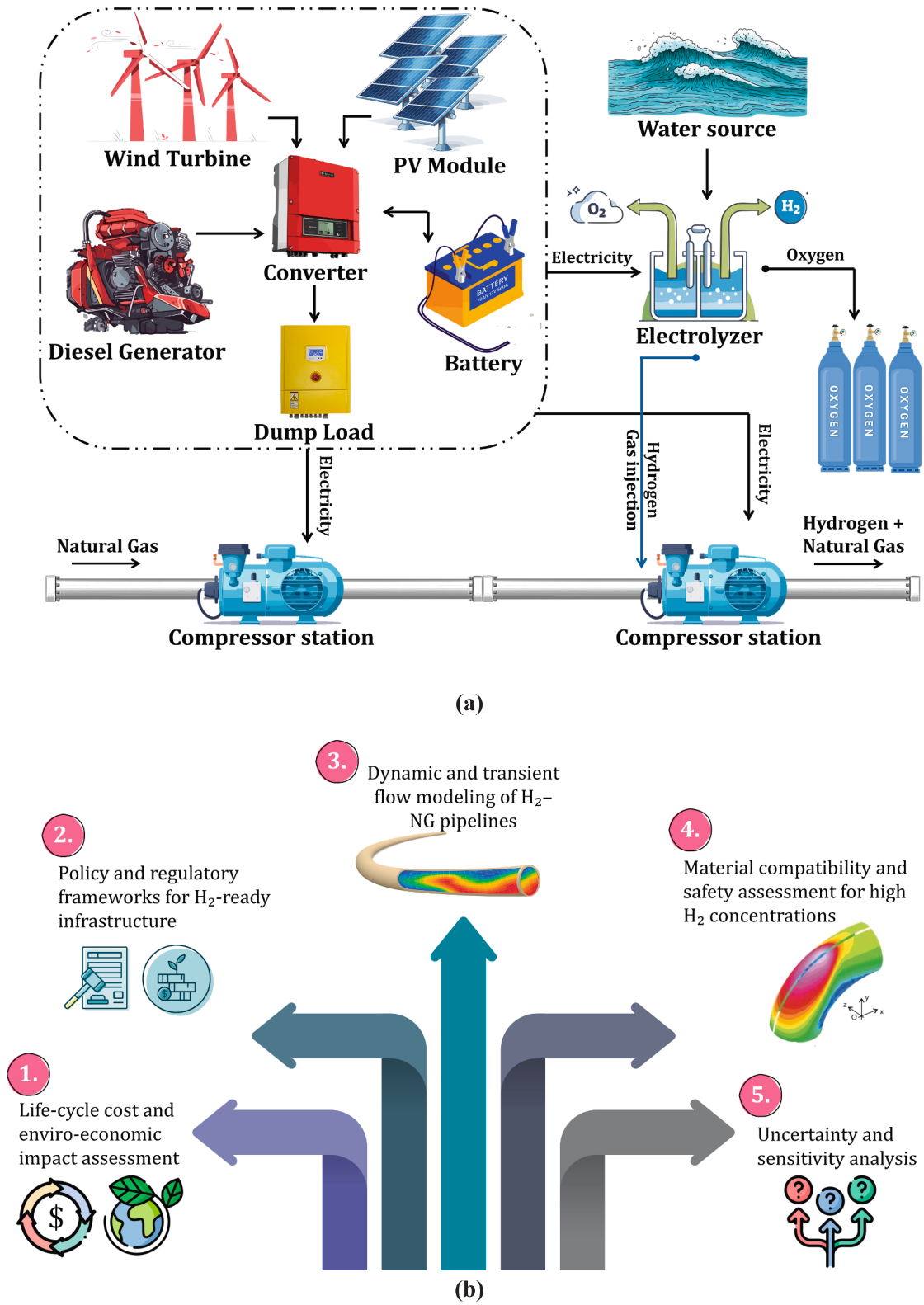

Fig. 23. **(a)** The schematic shows a novel and integrated framework for the electrification of NG pipeline compressor stations using renewable energy sources, **(b)** proposed future research directions.

framework.

- In large-scale natural gas transmission systems, operating conditions are typically maintained within narrow ranges over long periods. Transient effects (e.g., due to load fluctuations or compressor start-up and shutdown cycles) typically occur over shorter time horizons when analyzing annual-scale performance. Thus, steady-state modeling is a well-accepted approximation for evaluating long-term operational efficiency, energy return on investment, and emissions. Validation against benchmark studies confirmed < 1.5 %

deviation in key outputs, supporting the robustness of this framework for system-level techno-economic and environmental assessments. Nonetheless, future work should incorporate transient and non-isothermal dynamics to enhance real-world representativeness.

- While this study focuses on the techno-economic and environmental aspects of H_2 blending, ensuring material compatibility remains a fundamental prerequisite for translating these findings into practical deployment. H_2 at elevated concentrations can introduce several degradation mechanisms in existing steel pipeline infrastructure, including embrittlement, fatigue crack growth, and accelerated corrosion. These effects arise primarily due to H_2 diffusion into the metallic lattice, which reduces ductility, toughness, and fracture resistance of pipeline steels. As such, although the modeling framework explores blending scenarios up to 100 % H_2, in reality, the safe operating envelope of existing pipelines would be restricted by metallurgical limitations, weld integrity, and component-level compatibility (e.g., valves, seals, and compressor blades). Therefore, before transitioning to high-percentage H_2 blends, a comprehensive material compatibility assessment, including experimental testing of pipeline steels under pressurized H_2, fracture mechanics analysis, and accelerated aging tests, must be conducted.
- Although the present study concentrates on transmission-scale pipeline systems, emerging research on distributed micro-Power-to-H_2 (P2H) configurations underscores significant opportunities for enhancing efficiency and flexibility at the distribution network level. Future research could extend the proposed framework to capture cross-scale interactions, linking large-scale H_2 blending with localized P2H deployment to optimize both bulk energy transport and distribution-level efficiency.
- A life-cycle cost accounts for both capital and operating expenditures, and an enviro-economic impact assessment is needed to provide a more comprehensive understanding of long-term feasibility and sustainability. Parallel to this, the development of policy and regulatory frameworks for H_2-ready infrastructure will be essential to ensure safe and standardized deployment across different jurisdictions. Finally, conducting uncertainty and sensitivity analyses will strengthen the robustness of the proposed frameworks by evaluating performance under varying demand, market, and environmental conditions. Together, these avenues will advance the scientific, economic, and policy foundations for large-scale H_2 integration into existing pipeline systems (Fig. 23 **(b)**).

7. Conclusion

In summary, this study develops and applies a comprehensive modeling framework to analyze the implications of H_2 blending in natural gas transmission systems. The results provide deep insights into the technical, economic, and environmental trade-offs associated with varying H_2 concentrations. Key findings from the optimization and case study analyses are summarized as follows:

- Hydrogen injection into NG pipelines significantly alters flow dynamics. For an 800 km pipeline, the maximum operating pressure increases from 6.9 MPa (100 % NG) to 8.2 MPa (100 % H_2), while the minimum pressure decreases from 2.9 MPa to 1.9 MPa, indicating higher pressure drops with increasing H_2 content.
- Fuel consumption by compressors increases with H_2 blending. At 800 km and 8 GW power delivery, fuel consumption rises from 2.98 % (NG) to 3.73 % (10 % H_2) and 4.43 % (20 % H_2). For 100 % H_2, consumption peaks at 21.4 %, emphasizing the need for energy-efficient compression strategies.
- Model validation against established literature demonstrates high technical accuracy, with pipeline outlet pressures for a 30-inch diameter and 500 km inter-compressor spacing showing excellent agreement: 26.9 bar in the present model versus 26.5 bar in the reference study. The minimal deviation ($<$1.5 %) confirms the model's robustness in simulating H_2-enriched gas flow conditions under varying operating parameters.
- In the Coastal GasLink case study, a constant mass flow rate of 431.3 kg/s is maintained down to 4 MPa MAOP. Below this, the flow drops sharply due to pressure constraints, and fuel consumption reaches 8.97 % at 4 MPa.
- Full electrification of compressor stations reduces emissions from 1570 ktCO_2/year (NG-based system) to 116 ktCO_2/year but increases operating costs from M$116.73/year to M$650.16/year, highlighting a trade-off between environmental performance and cost.
- Full electrification of compressors reduces emissions by 1.51 MtCO_2/year at an abatement cost of $352/tonne CO_2, which drops significantly under Canadian subsidy scenarios, making deep decarbonization economically viable.
- The proposed strategy contributes $\sim$ 0.4 % toward Canada's 2030 target of 402 MtCO_2e/year – 438 MtCO_2e/year, demonstrating the potential of infrastructure decarbonization in meeting national emission reduction commitments.
- Energy Return on Investment declines from 33.56 (100 % NG) to 4.67 (100 % H_2), indicating increased energy demand for compression as H_2 content rises, underscoring the need for efficiency-focused design in H_2 transition.

Overall, this work offers a robust decision-support framework to guide the transition toward low-carbon H_2 infrastructure while balancing system performance, cost, and sustainability objectives.

Funding Statement

This research was funded by the Natural Science and Engineering Research Council (NSERC), Canada.

9. Declaration of generative AI in scientific writing

An AI tool was used to check for grammatical errors during the preparation of this manuscript. The author(s) subsequently reviewed and revised the content as necessary and assumed full responsibility for the final publication.

CRediT authorship contribution statement

Pronob Das: . Md. Shahriar Mohtasim: Writing – original draft, Visualization, Investigation, Formal analysis. **Andrew Rowe:** Writing – review & editing, Supervision, Resources, Project administration, Funding acquisition, Conceptualization. **Peter Wild:** Writing – review & editing, Supervision.

Declaration of competing interest

The authors declare that they have no known competing financial interests or personal relationships that could have appeared to influence the work reported in this paper.

Acknowledgement

The authors gratefully acknowledge the financial support provided by the Natural Sciences and Engineering Research Council of Canada (NSERC) through the Alliance Grant program. We also extend our thanks to the Institute for Integrated Energy Systems (IESVic) for their continued support and collaboration.

Data availability

No data was used for the research described in the article.

References

[1] Das P, et al. *Modeling and optimization of a hydrogen blended natural gas transmission network: effect of compressor electrification*. Int J Hydrogen Energy 2025;127:497–510.
[2] Mohtasim MS, et al. *Hybrid renewable multi-generation system optimization: Attaining sustainable development goals*. Renew Sustain Energy Rev 2025;212:115415.
[3] Das P, et al. *A review of natural gas transportation pipeline optimization and progress towards hydrogen injection: challenges and advances*. Int J Hydrogen Energy 2025;124:102–22.
[4] Wang G, et al. *Review on the transport capacity management of oil and gas pipeline network: challenges and opportunities of future pipeline transport*. Energ Strat Rev 2022;43:100933.
[5] Chong ZR, et al. *Review of natural gas hydrates as an energy resource: prospects and challenges*. Appl Energy 2016;162:1633–52.
[6] Arya AK, et al. *Improving natural gas supply chain profitability: a multi-methods optimization study*. Energy 2023;282:128659.
[7] Gordon JA, Balta-Ozkan N, Nabavi SA. *Socio-technical barriers to domestic hydrogen futures: Repurposing pipelines, policies, and public perceptions*. Appl Energy 2023;336:120850.
[8] Cristello JB, et al. *Feasibility analysis of blending hydrogen into natural gas networks*. Int J Hydrogen Energy 2023;48(46):17605–29.
[9] Liu S, et al. *Optimizing large-scale hydrogen storage: a novel hybrid genetic algorithm approach for efficient pipeline network design*. Int J Hydrogen Energy 2024;66:430–44.
[10] Zhang B, et al. *Influence of hydrogen blending on the operation of natural gas pipeline network considering the compressor power optimization*. Appl Energy 2024;358:122594.
[11] Chebouba A, et al. *Optimization of natural gas pipeline transportation using ant colony optimization*. Comput Oper Res 2009;36(6):1916–23.
[12] Kazi SR, et al. *Modeling and optimization of steady flow of natural gas and hydrogen mixtures in pipeline networks*. Int J Hydrogen Energy 2024;54:14–24.
[13] *The Hydrogen Strategy*. [cited 2025 June]; Available from: https://natural-resources.canada.ca/energy-sources/clean-fuels/hydrogen-strategy.
[14] Razi F, Dincer I. *Challenges, opportunities and future directions in hydrogen sector development in Canada*. Int J Hydrogen Energy 2022;47(15):9083–102.
[15] Ghorbani B, et al. *Canada's Hydrogen Future: Innovations, policies, and Global Perspectives*. Energy Fuel 2025;39(16):7605–48.
[16] Roadmap to 2030. [cited 2025 June]; Available from: https://www2.gov.bc.ca/assets/gov/environment/climate-change/action/cleanbc/cleanbc_roadmap_2030.pdf.
[17] Fairbrother M, Rhodes E. *Climate policy in British Columbia: an unexpected journey*. Front Clim 2023;4:1043672.
[18] Mohammadi, H. and J. Saddler, *Biofuel policies used by IEA Bioenergy Task 39 countries: the transition to using the carbon intensity (CI) of biofuels to set targets*. Biofuels, Bioproducts and Biorefining.
[19] Arya AK, et al. *A multi-objective model for optimizing hydrogen injected-high pressure natural gas pipeline networks*. Int J Hydrogen Energy 2023;48(76):29699–723.
[20] Liu J, et al. *Analysis of hydrogen gas injection at various compositions in an existing natural gas pipeline*. Front Energy Res 2021;9:685079.
[21] Wang B, et al. *An MILP model for the reformation of natural gas pipeline networks with hydrogen injection*. Int J Hydrogen Energy 2018;43(33):16141–53.
[22] Wang B, et al. *High-yield synthesis of vaterite microparticles in gypsum suspension system via ultrasonic probe vibration/magnetic stirring*. J Cryst Growth 2018;492:122–31.
[23] Üster H, Dilaveroğlu Ş. *Optimization for design and operation of natural gas transmission networks*. Appl Energy 2014;133:56–69.
[24] Kazi, S.R., et al., *Stochastic finite volume method for uncertainty management in gas pipeline network flows*. arXiv preprint arXiv:2403.18124, 2024.
[25] Aliyev, I., *Modeling and analysis methods for early detection of leakage points in gas transmission systems*. arXiv preprint arXiv:2504.06809, 2025.
[26] Islam A, et al. *Hydrogen blending in natural gas pipelines: a comprehensive review of material compatibility and safety considerations*. Int J Hydrogen Energy 2024;93:1429–61.
[27] Sharma S, Sahir AH. *Natural Gas and hydrogen blending: a perspective on numerical modeling and CFD analysis for transient and steady-state scenarios*. Chem Prod Process Model 2025;20(1):129–58.
[28] Tong Z, et al. *Research on multi-objective optimal route selection method for natural gas transmission pipeline*. Journal of Pipeline Science and Engineering 2024:100250.
[29] Ogbe E, et al. *Optimizing Renewable Injection in Integrated Natural Gas Pipeline Networks using a Multi-Period programming Approach*. Energies 2023;16(6):2631.
[30] Wu X, et al. *Operation optimization of natural gas transmission pipelines based on stochastic optimization algorithms: a review*. Math Probl Eng 2018;2018(1):1267045.
[31] Liu, S., et al., *A Graph-Enhanced DeepONet Approach for Real-Time Estimating Hydrogen-Enriched Natural Gas Flow under Variable Operations*. arXiv preprint arXiv:2504.08816, 2025.
[32] Klopčič N, et al. *Refurbishment of natural gas pipelines towards 100% hydrogen—a thermodynamic-based analysis*. Energies 2022;15(24):9370.
[33] Galyas AB, et al. *Effect of hydrogen blending on the energy capacity of natural gas transmission networks*. Int J Hydrogen Energy 2023;48(39):14795–807.
[34] Vespasiano D, et al. *Hydrogen blending in natural gas grid: energy, environmental, and economic implications in the residential sector*. Buildings 2024;14(8):2284.
[35] Zhang H, et al. *Effects of hydrogen blending on hydraulic and thermal characteristics of natural gas pipeline and pipe network*. Oil & Gas Science and Technology-Revue d'IFP Energies nouvelles 2021;76:70.
[36] Vidas L, Castro R, Pires A. *A review of the impact of hydrogen integration in natural gas distribution networks and electric smart grids*. Energies 2022;15(9):3160.
[37] Tabkhi F, et al. *A mathematical framework for modelling and evaluating natural gas pipeline networks under hydrogen injection*. Int J Hydrogen Energy 2008;33(21):6222–31.
[38] Austin BT, Sumathy K. *Transcritical carbon dioxide heat pump systems: a review*. Renew Sustain Energy Rev 2011;15(8):4013–29.
[39] Hai W, Xiaojing L, Weiguo Z. *Transient flow simulation of municipal gas pipelines and networks using semi implicit finite volume method*. Procedia Eng 2011;12:217–23.
[40] Misconel S. *CO2 reduction potentials and abatement costs of renewables and flexibility options–a linear optimization approach for the German sector-coupled energy system until 2045*. Energ Strat Rev 2024;52:101323.
[41] Torrubia J, Valero A, Valero A. *Renewable exergy return on investment (RExROI) in energy systems. the case of silicon photovoltaic panels*. Energy 2024;304:131961.
[42] King CW. *Energy intensity ratios as net energy measures of United States energy production andexpenditures*. Environ Res Lett 2010;5(4):044006.
[43] Canada, G.B. *Air Quality Technical Data Report - LNG Canada Export Terminal*. 2014 [cited 2025; Available from: https://projects.eao.gov.bc.ca/api/public/document/5886905ee036fb0105768ab6/download/Air%20Quality%20Technical%20Data%20Report_Part01.pdf.
[44] Khan MA, Young C, Layzell DB. *The techno-economics of hydrogen pipelines*. Transition Accelerator Technical Briefs 2021;1(2):1–40.
[45] Yu Q, et al. *Techno-economic analysis of hydrogen pipeline network in China based on levelized cost of transportation*. Energ Conver Manage 2024;301:118025.
[46] *The first direct path for Canadian natural gas to global LNG markets*. [cited 2025 12 June]; Available from: https://www.coastalgaslink.com/.
[47] Canada, G.o. *Emission factors and reference values*. May 2024 [cited 2025 June]; Available from: https://www.canada.ca/en/environment-climate-change/services/climate-change/pricing-pollution-how-it-will-work/output-based-pricing-system/federal-greenhouse-gas-offset-system/emission-factors-reference-values.html.
[48] BC, F. *Compare FortisBC natural gas rates with gas marketers' rates*. 2025 [cited 2025 June]; Available from: https://www.fortisbc.com/services/natural-gas-services/customer-choice-buying-from-natural-gas-marketers/compare-fortisbc-natural-gas-rates-with-gas-marketers-rates.
[49] Canada, G.o. *Natural Resources Canada*. [cited 2025 June]; Available from: https://natural-resources.canada.ca/.
[50] canada, N.R. *Hydrogen strategy for canada*. [cited 2025 June 12]; Available from: https://natural-resources.canada.ca/sites/nrcan/files/environment/hydrogen/NRCan_Hydrogen-Strategy-Canada-na-en-v3.pdf.
[51] Canada, N.R. *Canada's National Adaptation Strategy: Building Resilient Communities and a Strong Economy*. 2025 [cited 2025 June]; Available from: https://natural-resources.canada.ca/.